Identifying genes required for *Saccharomyces cerevisiae* growth in mucin

Kevin Jay Belarmino Mercurio

Thesis submitted to the University of Ottawa
in partial fulfillment of the requirements for the
MSc degree in Biochemistry

Department of Biochemistry, Microbiology and Immunology
Faculty of Medicine
University of Ottawa

Abstract

The human gut microbiome is a vast ecosystem of microorganisms that play an important role in human metabolism, immunological function, and even inflammatory gut diseases. Metagenomics research on the human gut microbiome has demonstrated the presence of DNA from dietary yeast species like *Saccharomyces cerevisiae*. However, it is unknown if the *S. cerevisiae* detected in metagenomics studies is solely from dead dietary sources or if they can live and colonize the human gut like their close relative *Candida albicans*. While *S. cerevisiae* can adapt to low oxygen and acidic environments, it has yet to be explored whether it can metabolize mucin, the primary carbon source found in the mucus layer of the human gut. Mucins are large, gel-forming, highly glycosylated proteins that make up a majority of carbohydrate sources in the gut mucosa. This work determined that *S. cerevisiae* can utilize mucin as their main carbon source which results in a significant reduction in cell size. Additionally, an aspartyl protease named Yps7, part of a family containing known homologues to mucin-degrading *C. albicans* proteins in *S. cerevisiae*, is important for growth on mucin media. To further identify biological pathways required to grow optimally in mucin, both a transcriptome analysis on wild type cells (BY4743) and a chemogenomics screen was performed. In total, 2131 genes demonstrated significant differential expression in mucin media, and 30 genes upon their deletion impacted their growth on mucin. Both these screens suggest that mitochondrial function is required for proper growth in mucin, which was further elucidated by the change in mitochondrial morphology and oxygen consumption in yeast cells upon mucin treatment. Indeed, the uncharacterized open reading frame *YCR095W-A* is required for growth on mucin as the deletion mutant showed dysfunction in mitochondrial morphology and cellular respiration, further suggesting a potential role in mitochondrial function. Importantly, this project serves as the initial step towards establishing if our most common dietary fungus can survive in the mucus environment of the human gut.

Acknowledgements

I would like to thank my supervisor, Dr. Kristin Baetz, for the opportunity to work on this novel project in her laboratory. Her mentorship in technical, writing, oral communication and professionalism skills will be applied throughout my career.

I would also like to thank the former Research Associate in the lab, Dr. Sylvain Huard, who consistently provided research guidance throughout my degree. He played a substantial role in troubleshooting various experimental protocols as well as improving my technical skills.

I would next like to thank all past and present Baetz Lab members who have provided both scientific and morale support throughout this project: Dylan Singh, Dr. Trang Pham, Dr. Eugene Fletcher, Elizabeth Walden, Sarah Laframboise, Garrett Fairman, Sangavi Sivananthan and Hana Knill.

I would additionally like to thank other researchers who have helped out regarding experimentation or technical guidance: Genome Quebec and the Canadian Centre for Computational Genomics (C3G) for the RNA sequencing with data summary, the Stintzi Lab for RNA sample preparation, and the Harper Lab for mitochondrial function analysis on their Seahorse Flux Analyzer system.

I would like to further thank my Thesis Advisory Committee for their technical and professional guidance throughout this project: Dr. Alain Stintzi, Dr. Kin Chan and Dr. Damien D'Amours.

I would like to thank the funding sources of this project, for which made this research possible: the NSERC-CREATE in Technologies for Microbiome Science and Engineering (TechnoMiSE) Program and the Ottawa Institute of Systems Biology (OISB).

I would lastly like to thank my family for their motivation to follow my scientific passions. It is due to them that I am a curious explorer of the countless universal wonders.

Table of Contents

1.0 Introduction
1.1 The human gut microbiome……1
1.2 Gut fungi and *Saccharomyces cerevisiae*……2
1.3 Mucin……..4
1.4 *S. cerevisiae* response to carbon limitation……..7
1.5 The role of aspartyl proteases in the *S. cerevisiae* stress response……9
1.6 The interplay between mitochondrial function and carbon-limiting conditions……11
1.7 Hypothesis and aims……..13

2.0 Materials and Methods……...14

3.0 Results
3.1 *S. cerevisiae* can utilize mucin as a carbon source but reduces cell size…….23
3.2 The aspartyl protease Yps7 is important for *S. cerevisiae* growth on mucin……..25
3.3 Yps7 displays differences in subcellular localization in mucin medium compared to YPD and YP……27
3.4 Mucin induces cellular stress but Yps7 growth deficiency is not rescued after alleviating osmotic or cell wall stresses……27
3.5 RNA-sequencing demonstrates drastic transcriptome remodelling during growth in mucin and the importance of mitochondrial-associated genes……31
3.6 Chemogenomics screen showcases various essential biological processes during growth on mucin and highlights the importance of mitochondrial function……34
3.7 Mitochondria fission and biogenesis is induced upon deletion of *CCM1* and *YCR095W-A* during growth in mucin……37
3.8 Mitochondrial function is disrupted upon deletion of *YCR095W-A* during growth in mucin……..38

4.0 Discussion
4.1 Impact of mucin on growth and morphology……42
4.2 Aspartyl proteases like Yps7 are important but not involved in potential responses to cell wall integrity or osmotic stress under mucin conditions……...43
4.3 Impact of mucin on mitochondrial morphology and function……47

5.0 Conclusion……...51

6.0 References……52

7.0 Contributions of Collaborators……..61

8.0 Appendices……...62

9.0 Curriculum Vitae……75

List of Abbreviations

AMP	Adenosine monophosphate
ATP	Adenosine triphosphate
BP	Base pair
cDNA	Complementary deoxyribonucleic acid
CT	Cycle threshold
DMA	Deletion Mutant Array
DNA	Deoxyribonucleic acid
FDR	False discovery rate
FPKM	Fragments per kilobase of transcript per million mapped reads
G418	Kanamycin
Gal	Galactose
GalNAc	N-acetyl galactosamine
GFP	Green fluorescent protein
GI	Gastrointestinal
GPI	Glycosylphosphatidylinositol
HYG	Hygromycin
ITS1	Internal transcribed spacer 1
LEU	Leucine
MAPK	Mitogen-activated protein kinase
mRNA	Messenger ribonucleic acid
NAG	N-acetyl glucosamine
NAT	Nourseothricin
OD600	Optical density at 600 nm
PBS	Phosphate buffer saline
PCR	Polymerase chain reaction
qRT-PCR	Quantitative real-time polymerase chain reaction
rRNA	Ribosomal ribonucleic acid
SAP	Secreted aspartyl protease
SC	Synthetic complete
SD	Synthetic dropout
SD-Leu	Synthetic dropout missing leucine (with 2% dextrose)
SDS-PAGE	Sodium dodecyl sulfate polyacrylamide gel electrophoresis
SM-LEU	Synthetic dropout missing leucine (with 0.5% mucin)
TCA	Trichloroacetic acid
TCCF	Total corrected cell fluorescence
UV	Ultraviolet
WCE	Whole cell extract
YNB	Yeast nitrogen base
YP	Yeast peptone
YPD	Yeast peptone dextrose
YPE	Yeast peptone ethanol
YPM	Yeast peptone mucin
Yps	Yapsin

List of Figures

Figure 1 Overview of mucin protein structure……..6

Figure 2 Overview of Yapsin (Yps) functions……10

Figure 3 *S. cerevisiae* can metabolize mucin as a carbon source but reduces cell size……24

Figure 4 *YPS7* gene expression is induced upon mucin exposure and *yps7*Δ cells display reduced growth on mucin……26

Figure 5 Yapsin proteins were diffused throughout the cell in YPM and only Yps7 is induced in mucin media……28

Figure 6 Mucin induces cellular stress, but *yps7*Δ growth deficiency is not rescued after alleviating osmotic or cell wall stresses……30

Figure 7 Gene ontology analysis for upregulated and downregulated genes are enriched for gene products involved in mitochondrial function and the cell cycle……...35

Figure 8 Distinct chemogenomic profile for *S. cerevisiae* growth on mucin comparing to growth on YP……..36

Figure 9 Mucin changes mitochondrial morphology and deletion of *CCM1* or *YCR095W-A* lead to increased Cit1-RFP in mucin media……39

Figure 10 Oxygen consumption rate (OCR) increases in the presence of mucin and disrupted upon deletion of *CCM1* or *YCR095W-A*……...41

Supplemental Figure S1 *S. cerevisiae* can grow and temporarily adapt to mucin media……...62

Supplemental Figure S2 *BAR1* displayed the lowest difference in gene expression between YP and YPM……63

Supplemental Figure S3 Yapsin proteins are mixed in regard to abundance in mucin media……64

Supplemental Figure S4 Principal component analysis (PCA) and transcriptional profiling demonstrate separation by sample treatment and a large set of differentially expressed genes……65

Supplemental Figure S5 Dot assay confirmations for the chemogenomics screen……66

List of Tables

Table 1 Top 50 upregulated genes in YPM compared to YP ranked by fold change……...32

Table 2 Top 50 downregulated genes in YPM compared to YP ranked by fold change……..33

Supplemental Table S1 Strain list…….68

Supplemental Table S2 Plasmid list……..70

Supplemental Table S3 Primer list……71

Supplemental Table S4 Top screen hits resulting in a positive impact on growth in YPM compared to YP upon their deletion…….73

Supplemental Table S5 Top screen hits resulting in a negative impact on growth in YPM compared to YP upon their deletion……74

1.0 Introduction

1.1 The human gut microbiome

The human gut microbiome is a vast community of microorganisms that are involved in the homeostasis of our gut physiology, metabolism and nutrient uptake, and even immune system functionality[1,2]. Since the Human Microbiome Project, many more data extensive studies focusing on the gut microbiome have been conducted to elaborate on how human genetics and microbial interactions affect our health[3–5]. These projects include highly regarded metagenomics initiatives like the European Metagenomics of the Human Intestinal Tract (MetaHIT)[6], the American gut microbiome analysis of lean and obese twins[7] and the Japanese gene ontology analysis of the gut microbiome[8]. The major finding from these hallmark studies was to not think of the microbiome in terms of only microbial composition, but also in terms of functionality. Individual microbial communities will vary yet still serve the functions of a healthy, stable microbiome.

Studies have shown that many gastrointestinal (GI) diseases have been correlated to microbial dysbiosis in the gut[1]. Microbial dysbiosis can be caused by many factors that include individual genetics, diet, pharmaceutical usage and disease[9,10]. In fact, the recent upsurge of metagenomics research in this field, in which DNA is extracted from faecal or gut biopsy samples, has focused on the correlations between gut microbiota and human disease[11]. It is the stable balance of many different microorganisms in the gut that lead to overall good health. Similarly, changes in the levels of specific microorganisms or a combination of microorganisms have been associated with disease[9]. Hence, it is critical that we understand the microbiome composition of both the healthy and diseased gut.

1.2 Gut fungi and *Saccharomyces cerevisiae*

Although mainly focusing on bacteria, the development of high-throughput metagenomics has also led to research on the fungal community within the gut in relation to the impact of diet and pathogenesis[12–16]. Our collection of fungal microbiota (ie. mycobiome) are typically characterized as either residing within/on the human body (indigenous) or taken up from the environment (exogenous). This is important as it explains the variability observed in all microbiome studies, due in large part to the geographical location and dietary regimens of the studies' cohorts[17,18].

Currently, and unlike the bacteriome, there is no consensus on a core mycobiome, nor a consensus on the symbiosis between gut fungi and the host. However, research has aimed to determine what gut fungal species healthy individuals possess by using sequencing methods that focus on conserved regions of ribosomal RNA in the 18S or internal transcribed spacer 1 (ITS1) regions. One metagenomics study by Nash *et al.* (2017)[19] extracted DNA from stool samples of 147 healthy volunteers over the course of one year, looking at both conserved regions. Despite high variability between volunteers among the core species comprising their mycobiomes, *Saccharomyces cerevisiae*, *Malassizia restricta* and *Candida albicans* were detected in each individual volunteers' samples among 92.2%, 78.3% and 63.6% of all 147 volunteers, respectively. This suggests that these three species may be resident microbes in the human GI tract and interact with the overall gut microbiome. Another study by Strati *et al.* (2016)[20] took both culture-dependent and culture-independent approaches to determine a core mycobiome among 111 healthy subjects and changes due to age and gender. Although no significant differences were observed in fungal population among age groups (excluding higher richness through ITS1 sequencing in infants and children compared to adults), there was a higher number of fungal isolates and fungal diversity in female volunteers compared to male volunteers. As previously stated, metagenomic studies

cannot differentiate between live fungi residing in the gut or dead fungal remnants from the environment as the cause for the detection of specific fungal species in these studies[17,19].

However, it is believed that fungi have an important role in human health. For example, research has been conducted on *Saccharomyces boulardii* as a probiotic additive in the food industry, as well as a medical treatment for diarrhea, cholera and inflammatory bowel disease[21]. Interestingly, in a 2015 review of gut microbiome publications, only 15 fungal species were reported in five or more studies[22]. The most commonly reported in these studies were the closely related *Candida spp*. and *Saccharomyces spp*. *Candida albicans* is the most frequently studied fungus regarding the impact of the mycobiome on human health because of its virulent ability in immunocompromised individuals[23,24]. But despite being one of the most abundant fungi in most human diets, *Saccharomyces cerevisiae* (ie. budding yeast) has been often overlooked by *C. albicans* during discussions of microbial impact within diseased individuals.

S. cerevisiae is one of the most common dietary fungi due in large part to its utilization during the production of bread and alcoholic beverages by fermentation[25,26]. Regarding the role of *S. cerevisiae* in human health, research still remains inconclusive. *S. cerevisiae* is known to reduce symptoms of enteritis/colitis in mice and humans[16,21,27,28]. Conversely, *S. cerevisiae* was shown to increase intestinal damage and permeability when inoculated in germ-free mice, due to the enhancement of host purine metabolism and induction of uric acid synthesis[29]. Though the latter study uses unrealistic inoculation of yeast via oral gavage, the idea that dietary yeast will always be a commensal organism within a host remains to be determined.

Current high-throughput culture-independent studies for determining fungal composition have typically discovered *S. cerevisiae* in stool samples[12–16,30], with only two studies detecting *S. cerevisiae* from mucosa samples by polymerase chain reaction (PCR)[31,32]. This finding does not conclude whether identified *S. cerevisiae* genetic material came from colonized cells in the human

gut, or dead/dormant cells passing through the GI tract. Most recently, faecal samples taken from infants immediately after birth were cultured with fungal selection drugs and found identifiable aerobic and anaerobic fungi in 31% and 39% of all infants, respectively[33]. In another study, researchers have looked at the shift in mycobiota between eutrophic, overweight and obese individuals[34]. Stool samples from healthy individuals from various age groups have also been analyzed both through culture-dependent and culture-independent methods, tied with phenotypic assays to determine fungal isolates adaptability to gut conditions[20]. As early as 2015, researchers have looked at fungal composition of the human microbiome in a culture-dependent manner, seeking differences in lung microbial communities between healthy individuals and patients afflicted with cystic fibrosis[35]. However, all culture-dependent studies have admitted the difficulty in obtaining conclusions due largely to the lack of reproducibility of culture-dependent analyses, emphasizing very little on the exact species identified.

It remains to be determined if the *S. cerevisiae* identified in any metagenomic studies reflect colonized or dead yeast. Yet, for any organism to survive in the gut, they must be able to adapt to gut conditions such as low oxygen content[36], slightly acidic pH[37], body temperature, and a mucus-rich environment[38]. While *S. cerevisiae* is known to adapt to low oxygen and acidic environments, it is currently not known whether it can live off the resources found in the mucus layer of the human gut.

1.3 Mucin

The epithelium of the gut is covered in a mucus layer that serves to lubricate the passage of food, as well as to protect host cells from intestinal damage and pathogen invasion[38]. This layer is composed of water, salts, immunoglobulins, secreted proteins and mucin[39], the latter constituting

the most abundant supply of carbohydrates found in the gut. Mucins are large, gel-forming, highly glycosylated proteins ranging from 200 – 200,000 kDa in size[40]. These proteins are usually protected from proteases in the environment due to the large abundance of O-linked oligosaccharides surrounding the protein core[38,40]. Upon initial glycosylation, 10 or more sugar moieties can be further attached, leading to a large heterogeneric network of galactose, fucose, N-acetyl galatacosamine and N-acetyl glucosamine[41]. A schematic overview of mucin structure can be found in Figure 1.

Mucin plays an important role in the gut environment. In the colon, the crypt goblet cells are responsible for secreting these proteins that reinstate the barrier[42–44]. Structurally, there are two types of mucin glycoproteins: transmembrane mucins (ex. Muc1, Muc4) that are anchored to epithelial cells, and gel-forming mucins (ex. Muc2, Muc5AC) that are excreted to form large, densely packed polymers. These dense glycoproteins also retain water, and upon linkage causes its gel-like property[43,44]. Both types serve their purpose in the colon, which is known to have a dual layer system. As the inner layer mucins remain firmly attached and serve to protect the intestinal membrane, the outer layer is loose and allows microbes to reside[45]. This outer layer is possible due in part to cleavages of Muc2 mucin without disrupting the polymeric gel network[45].

There are several studies that replicate the mucus layer of the human epithelium, namely using *Pseudomonas aeruginosa* for research on cystic fibrosis[46–48] or *Candida albicans* for research on candidiasis[49,50]. Unsurprisingly, research on fungi characterization in mucin media has mainly focused on *C. albicans*. Upon exposure to mucin in liquid media, *C. albicans* cells were observed to have unicellular ellipsoidal morphology rather than their typical hyphae or distinct round yeast structure[49]. Interestingly, *C. albicans* has the unique virulence ability to switch among various cellular morphologies, therefore masking detection by the host until conditions favour its switch to its virulent hyphae form[50–53].

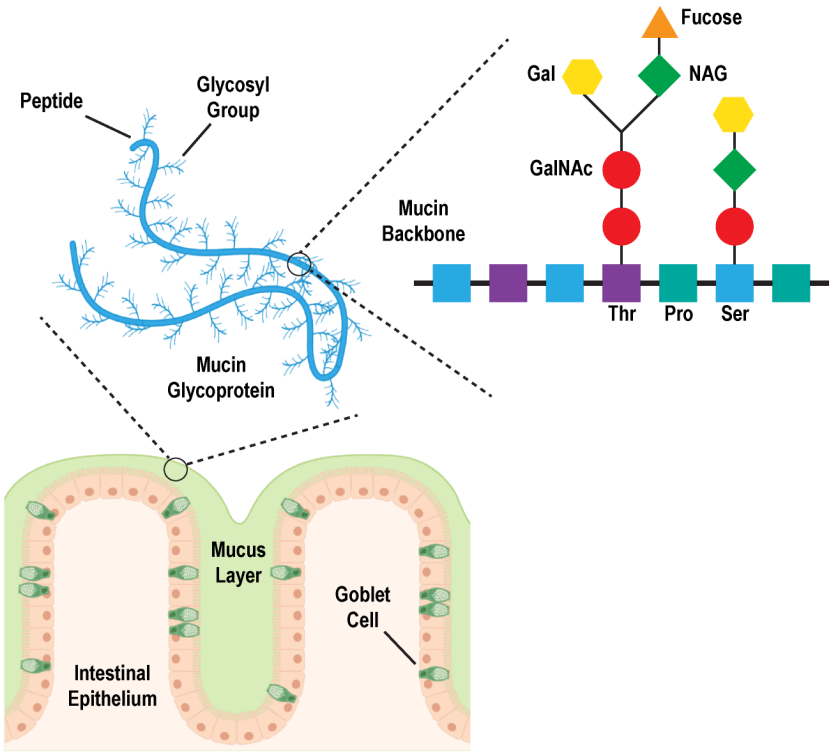

Figure 1 Overview of mucin protein structure. Colonic mucin is synthesized by goblet cells embedded in the intestinal epithelium and is the predominant contributer to the gel-like network that make up the mucus layer. The mucin backbone is comprised of repeated proline, threonine and serine residues. N-acetyl galactosamines (GalNAc) are O-linked to serine or threonine residues that can extend via the addition of other sugar moieties like N-acetyl glucosamine (NAG), galactose (Gal) and fucose. Figure is derived from Johansson *et al.* (2013).

Unlike *C. albicans*, it is presently not known if *S. cerevisiae* can utilize mucin glycopolymers as an energy source to live within oxygen-limiting, mucus niches such as those found within the gut, nor is it known if the *S. cerevisiae* detected in metagenomics studies are reflective of live yeast living in the gut.

1.4 *S. cerevisiae* response to carbon limitation

In the environment and even industrial food processing, researchers have been interested in the response to nutrient limitation by *S. cerevisiae*[54]. It is commonly reported that in various nutrient-deprived conditions, repression was observed for genes involved in ribosomal biogenesis and protein translation[55,56]. Sensing nutrients in the environment also plays a factor in the overall response to nutrient limitation, including transcriptional regulation. Growth rate dependent organization of the transcriptomic response was shown to be mainly determined by cell sensing of environmental nutrients, and the activation of PKA-dependent signalling cascades[57,58]. However, due to the structure of mucin, it is unknown whether sensors for carbon or nitrogen sources in the environment are key to yeast survival in the gut. Just like how the food and beverage industry has taken keen interest in yeast adaptation to nutrient-deprivation[59]; when regarding an environment as limiting as the human gut, it is important to understand the transcriptomic changes that may occur.

Under carbon or glucose limiting conditions, genes involved in the tricarboxylic acid cycle, oxidative phosphorylation and oxidative stress were upregulated, while low/moderate affinity hexose transporters and cell proliferation were downregulated[60,61]. Another prominent gene known to be activated under carbon-limiting conditions is *SNF1*, encoding an AMP-activated kinase known to promote respiratory metabolism, glycogen accumulation, gluconeogenesis, autophagy and the glyoxylate cycle[62]. Regarding nutrient sensing, glucose sensing is conducted via the

interactions of the Snf3-Rgt2 regulatory complex, the Snf1-Mig1 glucose repression pathway and the Ras-cAMP pathway[63]. Moreover, amino acid sensing by the Ssy1-Ptr3-Ssy5 system induces the synthesis of amino acid transporter genes and subsequent amino acid metabolism[64].

In terms of morphology, both *C. albicans* and *S. cerevisiae* cells can transition from their single-cell budding yeast form into multicellular filaments, allowing for invasive or pseudohyphal growth in response to different nutrient-limiting conditions[65–67]. Regulation of these pathways are dependent on cAMP-PKA and MAPK pathways involved in nutrient sensing[67,68]. An important protein activated in both pathways is Flo11, a cell surface protein that mediates filamentous growth[69]. This protein, along with the histone deacetylase complex, the Rim101 signalling pathway and other transcriptional regulators like Mit1, Tec1, Flo8 and Mss11 are essential for activation of filamentous growth[70]. Another critical protein in the activation of filamentous growth during carbon limitation is Msb2, a glycoprotein and glucose sensor at the plasma membrane[71]. Although the mechanism by which Msb2 senses carbohydrates like glucose in the environment is not entirely known, the cleavage of its extracellular domain by the aspartyl protease Yps1 has been found to be required for overall filamentous growth[72]. Another MAPK protein that is associated with aspartyl proteases is Hog1, one of the primary signalling proteins involved in the hyperosmotic stress response. Hog1 regulates glycerol synthesis to combat hyperosmotic conditions[73] and osmoresponsive transcription factors like Msn2/Msn4, Hot1, Sko1/Acr1, Smp1, which are essential for various stress responses[74]. There is evidence for aspartyl proteases like Yps7 interaction with proteins specific to the *HOG1* mitogen-activated signalling pathway like Ssk2[75]. These interactions between signalling proteins of the PKA and MAPK pathways, along with the proteolytic activity of plasma membrane proteins, permit yeast cells to optimize resources in nutrient limiting environments by changing their transcriptome and cellular morphology.

1.5 The role of aspartyl-proteases in the *S. cerevisiae* stress response

Some fungi have proteins that allow them to break down mucin and live within the mucus layer of the gut. For example, extensive research on *C. albicans* has demonstrated the importance of a family of 10 secreted aspartyl proteases (SAPs) for fungal pathogenicity[76]. Aspartyl proteases work optimally under acidic pH to cleave peptides using two aspartic acid side chains in their catalytic domain[77]. Gene expression of SAPs have been associated with adhesion and hyphae formation[53,78]. SAPs also contribute to virulence by breaking down host defense mechanisms, such as the natural antimicrobial peptide histatin 5[79,80], the integral E-cadherin found among epithelial cell junctions[81], and the protective mucosal barrier[82].

Interestingly, the significance for breakdown of the mucosal barrier does not seem to be only for supporting penetration. One study has shown that *C. albicans* has the ability to utilize mucin as the major carbon and nitrogen source in liquid and solid media[82]. Although the mechanism is still not clear, Sap2 western blot detection and biotin-labelled mucin degradation on a zymogram demonstrated the importance of this particular SAP for mucin breakdown, coinciding with research on clinical isolates of *C. albicans*[82,83].

S. cerevisiae shares 90% of its genome with *C. albicans*[84], including protein homologues to SAPs named Yapsins (Yps), a family of aspartyl proteases. There are six known Yps proteins, of which only Yps1, Yps2 and Yps3 are characterized on the *Saccharomyces* Genome Database (https://www.yeastgenome.org/). A schematic overview of known and hypothesized functions for Yps proteins can be found in Figure 2. Regarding peptide sequence, Yps1, Yps2 and Yps3 share 50% sequence identity, while Yps6 more closely resembles Bar1 (an aspartyl-protease involved in pheromone response), and Yps7 more closely resembles Pep4 (a vacuolar protease involved in the activation of other vacuolar proteases and plasma membrane transporters)[85]. Yps1 and Yps3 share

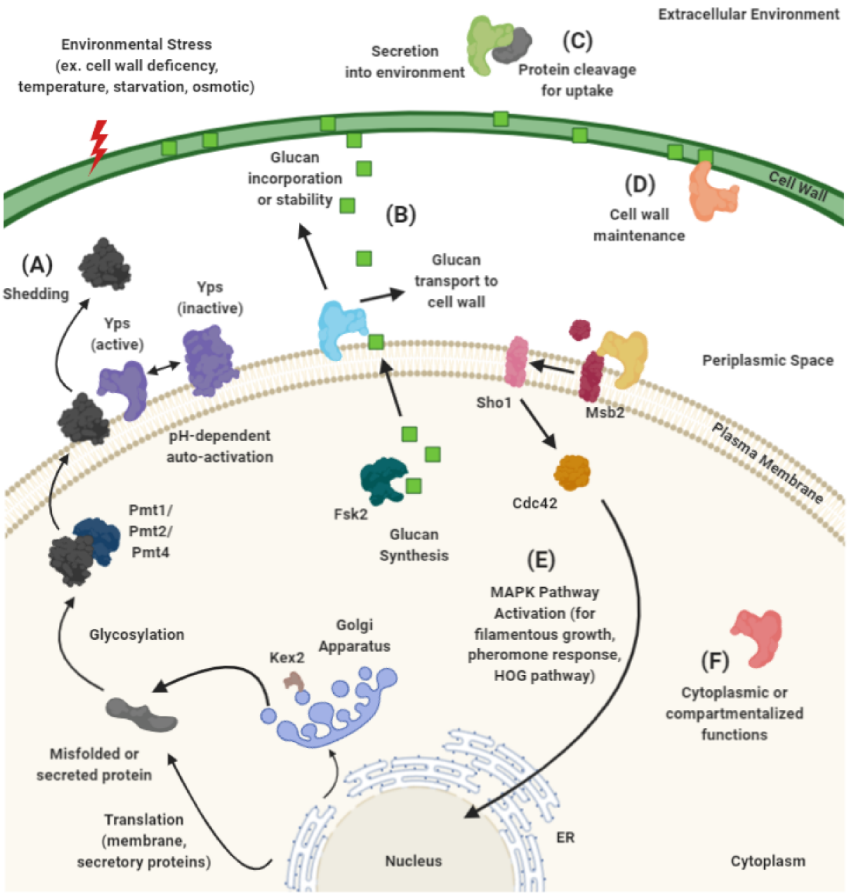

Figure 2 Overview of Yapsin (Yps) functions. Functions described have been confirmed or hypothesized based on protein sequence. Yps proteins are typically induced during times of environmental stress (ex. cell wall deficiency, temperature, starvation, osmotic, etc.). (A) *Shedding*. Membrane or secretory proteins are translated at the endoplasmic reticulum (ER) and undergo protein modifications in the cytoplasm or Golgi apparatus via the serine protease Kex2. Secreted or misfolded proteins that escape degradation are glycosylated by PMT proteins and sent to the plasma membrane. Yps proteins are pH-dependently auto-activated and cleave secreted or misfolded proteins at the cell surface. (B) *Glucan transport or incorporation/stability*. Cell wall stress leads to an induction in glucan synthesis by Fsk2. Some Yps proteins localized at the cell periphery are hypothesized to aid in transporting newly synthesized glucans to reinforce the cell wall, or incorporate and stabilize glucans directly at the cell wall. (C) *Extracellular protein cleavage for uptake*. Some Yps proteins are known to be secreted and break down proteins in the extracellular environment for potential resource scavenging. (D) *Cell wall maintenance*. Some Yps proteins are hypothesized to localize to the cell wall itself and maintain cell wall integrity through unknown mechanisms. (E) *MAPK pathway activation via Msb2*. Some Yps proteins are known to interact with the signalling mucin Msb2 by cleaving its ectodomain. This activates the protein and begins the signalling cascade from Sho1 to Cdc42, the latter of which can activate various MAPK signalling pathways for filamentous growth, pheromone response and hyperosmotic stress response. (F) *Cytoplasmic or compartmentalized functions*. Localization of Yps proteins is typically described at the cell periphery. This localization is governed by signalling peptides at the C-terminus of the protein. It is hypothesized that different conditions affect the signalling peptide, leading to uncommon localizations of Yps proteins for unknown functions.

the most amino acid sequence similarity to SAPs, with Yps3 showing the highest identity to *C. albicans* Sap2. Yps1 and Yps3, both glycosylphosphatidylinositol(GPI)-anchored proteases, have been shown to be most functional at pH 5-6[85,86], similar to the average pH of the human colon[37]. Moreover, Yps3 was shown to be a highly glycosylated protein, which may be attributed to the regulation of its secretion by the cell upon cleavage of the GPI-anchoring signal at its C-terminus[85,87], similar to Sap2 secretion by *C. albicans*.

The majority of research on Yps proteins focus on their potential role in cell wall integrity[88,89]. Interestingly, for uncharacterized Yps7, the synthetic lethality phenotype observed within *slt2*Δ*yps7*Δ cells suggests a compensatory role for loss of the *PKC1-SLT2/MPK1* cell wall maintenance pathway[90]. Other studies have looked at the ability of Yps proteins' to target misfolded GPI-anchored proteins for degradation[86,91]. Furthering on their involvement in protein degradation, they have even been demonstrated to cleave proteins in the external environment, which is an issue in the industrial production of recombinant proteins using *S. cerevisiae*[92]. Altogether, their potential role in resource collection by mucin degradation and mucosal resource uptake by their involvement in stress response pathways like cell wall maintenance has yet to be explored.

1.6 The interplay between mitochondrial function and carbon-limiting conditions

The mitochondrion is extremely important for eukaryotic cells to extract energy from environmental resources. In *S. cerevisiae*, there are four main complexes along the inner mitochondrial membrane that constitute the electron transport chain which, along with reducing agents produced in the tricarboxylic acid cycle, conclude with the synthesis of adenosine triphosphate (ATP) through oxidative phosphorylation[93]. *S. cerevisiae* also possesses the ability to

satisfy its energy requirements by fermentation, a cytoplasmic process that generates ATP by converting specific (fermentable) carbon sources to ethanol[94]. Although some genes are located within the mitochondrial genome, most mitochondrial associated genes are located in the nucleus, which encode for proteins involved in activation of mitochondrial translation and the tricarboxylic acid cycle, as well as the synthesis of mitochondrial structural proteins[95–97]. This is important as protein sorting of the 15-20% of all proteins into the mitochondria is essential for proper cellular function[98]. Under normal conditions, mitochondria form tubular networks along the cell cortex, whose integrity is balanced by fusion and fission events dependent on cell growth and extracellular cues[99–101]. These many processes all occur simultaneously to ensure proper functionality of the organelle during the yeast cell cycle.

S. cerevisiae has become a standard model organism for studying both mitochondrial function and dynamics under different conditions and genetic backgrounds[95,100]. It is known that mitochondrial ultrastructure, internal membrane organization, protein synthesis and mitochondrial-associated gene transcription can drastically change depending on the cell's functional state[102]. In turn, these affect the overall morphology of the mitochondria. For example, respiring yeast have been shown to increase synthesis of mitochondrial proteins by 10-20 fold compared to non-respiring yeast, which also leads to a 3-fold increase in mitochondrial size[55].

The mitochondrion of *S. cerevisiae* has been studied under various nutrient-limitation conditions. Adaptation of the yeast cell through structural and functional changes permit the most efficient growth under stressful conditions. Studies have shown that under stress, fission and mitophagy is often induced[103]. Yeast cells grown in nitrogen-limiting media with fermentable carbon sources demonstrate rapid mitochondrial turnover[104]. Conversely, yeast cells grown in nitrogen-limiting media with non-fermentable carbon sources showcase low amounts of mitophagy[104]. Studies have also shown inhibition of mitochondrial degradation when deleting

HOG1 or *SLT2* genes involved in the MAPK signalling pathway for osmotic and cell wall stress[105], conditions which can be similar to yeast grown in the presence of media containing thick mucin glycoproteins. In glucose-limiting conditions, aerobically grown yeast cells demonstrate strictly respiratory glucose metabolism, as well as have short and round mitochondria similar to those of yeast grown in ethanol[106]. Interestingly, yeast cells grown anaerobically under glucose-limiting conditions demonstrate strictly fermentative glucose metabolism, as well as have large, branched mitochondria similar to those of yeast grown in non-limiting glucose[106]. These differences in mitochondrial dynamics could potentially elucidate how *S. cerevisiae* may grow in the mucus environment of the gut.

1.7 Hypothesis and aims

I hypothesize that *Saccharomyces cerevisiae* can grow in a mucin environment, with changes in gene expression impacting cell structure and metabolism. I pursued two different aims for this project:

Aim 1: To determine whether *S. cerevisiae* can utilize and adapt to metabolizing mucin.

Aim 2: To identify pathways required for *S. cerevisiae* growth in mucin.

2.0 Materials and Methods

2.1 Yeast strains, plasmids, primers and media

All yeast strains, plasmids and primers used in this study are listed in Table S1, Table S2 and Table S3, respectively. Strains that were created for this project were generated by the PCR-mediated deletion and modification of chromosomal genes protocol outlined in Longtine *et al.* (1998)[107], and confirmed via growth on drug selection (G418, NAT, HYG [Multicell]) or nutrient deprivation, and PCR. Other strains were taken from the *Saccharomyces cerevisiae* Deletion Mutant Array[108] (GE, CAT#YSC1053) and GFP collection[109] (Thermo, CAT#95702). Cells were grown in standard yeast-peptone media created using final concentrations of 10 g/L yeast extract (Multicell), 20 g/L bacteriological peptone (Multicell), and 0.33 g/L of L-tryptophan (Sigma-Aldrich); or synthetic media (synthetic complete [SC] or synthetic dropout [SD]). All synthetic media were created using 6.7 g/L of yeast nitrogen base (YNB) with ammonium sulfate (Multicell) and 2.06 g/L of standard amino acid mix (for SC) or dropout mix (for SD). Water-soluble carbon sources were added after autoclave sterilization at final concentrations of 2% dextrose (YPD) and 0.5% Type III porcine gastric mucin (YPM) (Sigma-Aldrich, M1778). Mucin was partially purified as described by Glenister *et al.* (1988)[110], and stock solutions were further sterilized by autoclave similarly to Terra *et al.* (2010)[111] at 121°C for 15 min. Agar plates were created using a final concentration of 20 g/L agar (BioShop) added prior to autoclave. For sorbitol dot assays, media plates were created using a final concentration of 1M sorbitol added prior to autoclave.

2.2 Dot assays

Strains were grown overnight at 30°C in YPD. Cultures were then re-inoculated into 5 mL of YPD to an OD600 of 0.1 and incubated at 30°C. Once they reached log phase, cultures were washed twice in YP or SD (no dextrose), diluted to an OD600 of 0.2 in YP or SD as indicated. Dot assays were performed by spotting 3 uL of 10-fold serial dilutions (OD600 = 0.2, 0.02, 0.002, 0.0002) on indicated media plates and incubated for 2-6 days at indicated temperatures, depending on the assay. Images of dot assays were taken using the Bio-Rad Chemidoc™ XRS system under EPI-white light illumination and ImageLab software.

2.3 Time course growth and morphological assessment

Diploid (BY4743) strain was grown overnight at 30°C in YPD. Cultures were then re-inoculated into 50 mL of YPD to an OD600 of 0.1 and incubated at 30°C. Once they reached log phase, cultures were washed twice in YP and resuspended in 10 mL of YP. Cell suspensions were diluted to an OD600 of 0.1 in 50 mL of indicated media and incubated for six days at 30°C. On each day, 100 uL was aliquoted from each culture for cell counting on a hemocytometer under a standard light microscope. Additionally, 5 mL was aliquoted from each culture, spun down and resuspended in SC (no dextrose) for brightfield imaging (0.006s exposure time, 100% gain) using the Leica DMI 6000 fluorescent microscope (Leica Microsystems GmbH, Wetzler, Germany) equipped with a Sutter DG4 light source (Sutter Instruments, California, USA), Ludl emission filter wheel with Chroma band pass emission filters (Ludl Electronic Products Ltd., NY, USA) and Hamamatsu Orca AG camera (Hamamatsu Photonics, Herrsching am Ammersee, Germany).

2.4 RNA extraction

Diploid (BY4743) strain was grown in triplicate in 50 mL of YPD at 30°C to log phase. Once they reached log phase, cultures were washed twice in YP and resuspended in 10 mL of YP. Cell suspensions were diluted to an OD600 of 0.1 in 100 mL of YP and YPM, and incubated until log phase (one day) at 30°C. Cell counts were performed as previously described in order to normalize each sample at harvest. Cells were washed in dH2O, transferred to 2 mL screw-capped tubes and pellets were flash frozen in liquid nitrogen. Pellets were resuspended in 200 uL of breaking buffer (2% Triton X-100, 1% SDS, 100 mM NaCl, 100 mM Tris-HCl [pH8.0], 1 mM EDTA) and 200 uL of a phenol:chloroform:isoamyl alcohol mixture (125:24:1, pH 4.5) (Thermo, CAT#AM9720) was added to each sample. 0.5 mm glass beads (BioSpec, CAT#11079105) were added to just under the sample meniscus, and tubes were vortexed for 3.5 min. Samples were centrifuged at max speed for 25 min at 4°C, and the aqueous phase was aliquoted into a clean 1.5 mL microcentrifuge tube. Total RNA was ethanol precipitated out of solution and resuspended in nuclease-free water. Three DNase treatments using DNaseI (Promega, CAT#M6101) for one hour at 37°C were performed to remove genomic DNA, and subsequently purified using the RNA Clean and Concentrator-25 kit (ZymoResearch, CAT#R1017). RNA integrity was assessed by gel electrophoresis using a 0.8% agarose gel. RNA purity was assessed through two different ways: 1) the Thermo Scientific Nanodrop 2000 spectrophotometer and 2) Agilent Bioanalyzer RNA 6000 Nano quantification kit, the latter used specifically for RNA-sequencing (Agilent, CAT#5067-1511).

2.5 qRT-PCR

RNA samples were converted to cDNA using the iSCRIPT cDNA synthesis kit (Bio-Rad, CAT#170890). All primers (see Table S3) used for qPCR were obtained from ThermoFisher and evaluated for their efficiency by conducting qPCR on pooled cDNA samples. Primers are as follows: 1) *BAR1* F: 5'-AGGAGATGTATTACGCAACA-3', R: 5'-GGTAAGCAGAAGGGATTGCT-3'; 2) *YPS1* F: 5'-CATCGCAGGTTCTCGGTAAG-3', R: 5'-CTAGCGAGTCCCCGTAAAGC-3'; 3) *YPS2* F: 5'-GATGATTACGAGCTGGTGGA-3', R: 5'-TGTCGACAAGCACAGTAACT-3'; 4) *YPS3* F: 5'-AGCAGTCTTAACTAGTCCGG-3', R: 5'-TCGATCTCTTGCTGAGTTCA-3'; 5) *YPS5* F: 5'-GCTGACATTGCCTATTGCAA-3', R: 5'-GAGGTGGTAGTAGAACGAGG-3'; 6) *YPS6* F: 5'-GCATCTTGTTTGGTGCAGTG-3', R: 5'-ATCCCAGGATTTGAGCCAAG-3'; 7) *YPS7* F: 5'-GCAAAGTCTGGAACCTCTTC-3'; R: 5'-GTTGACCGGGAGTGCCAAAT-3'. Serial dilutions of 1:5 were used to determine the most optimal annealing temperature for each primer set. qPCR was performed using the SsoFast™ EvaGreen® Supermix (Bio-Rad, CAT#172-5201) and conducted on the BioRad CFX-96 using the standard two-step annealing procedure: 95°C for 3 min followed by 40 cycles of 95°C for 10 s, and 57°C for 10 s. Cycle threshold (CT) values were obtained and used for analysis. Fold changes were calculated using the ΔΔCT method[112] using the reference gene *BAR1*, which had the lowest difference in gene expression between YPM and YP media among the five candidates tested (Supplemental Figure S2). Three biological replicates and three technical replicates were used for each sample. Statistical analyses with the two-tailed unpaired t-test was performed for statistical significance with the GraphPad Prism software.

2.6 Protein lysate

GFP-tagged strains were grown overnight at 30°C in YPD. Cultures were then re-inoculated into 200 mL of YPD to an OD600 of 0.1 and incubated at 30°C. Once they reached log phase, cultures were washed twice in YP and resuspended back in 10 mL of YP. Cell suspensions were diluted to an OD600 of 0.1 in 500 mL of YP, YPM and YPD and incubated for one day at 30°C. Cell counts were taken in order to normalize cell harvests to the lowest concentrated culture. After harvest, cells were lysed using the trichloroacetic acid (TCA) procedure[113]. Briefly, cells were washed in 1 mL of ice-cold 20% TCA and pellets were flash frozen in liquid nitrogen. Cell pellets were subsequently resuspended back in 200 uL of ice-cold 20% TCA. 0.5 mm glass beads (BioSpec, CAT#11079105) were added to just under the sample meniscus, and cells were lysed mechanically by beadbeating. Cell debris and glass beads were removed by centrifugation. Whole cell extract (WCE) was resuspended in 400 uL of Laemmli loading dye (50 mM Tris [pH 6.8], 2% sodium dodecyl sulfate, 0.1% bromophenol blue, 10% glycerol, 100 mM β-2-mercaptoethanol) and stored at -80°C.

2.7 Quantitative western blotting

Prepared WCEs were boiled at 95°C for 10 min and separated by SDS-PAGE using the 10% TGX Stain-Free™ FastCast™ Acrylamide Kit (Bio-Rad, CAT #1610183) at 180V for 1.5 hours. Acrylamide gels were activated using the Bio-Rad Chemidoc™ XRS system under UV light and ImageLab software. Proteins were transferred onto a nitrocellulose membrane using the Bio-Rad Semi-Dry Trans-Blot Turbo™ Transfer System at 25V for 7 min. Membranes were visualized under UV light once again to measure total protein content in each lane. Blocking was performed

with 5% non-fat milk powder dissolved in phosphate buffer saline (PBS) with 1% Tween20 for two hours. Following this, membranes were incubated overnight at 4°C with GFP primary antibody (Sigma, CAT#11814460001). On the next day, membranes were washed with PBS-Tween three times and incubated with anti-mouse secondary antibody (Bio-Rad, CAT#170-6516) for two hours. Lastly, immunoblots were developed with Clarity™ Western ECL (Bio-Rad, CAT#170-5061) and protein bands were visualized with the Bio-Rad Chemidoc™ XRS system.

2.8 GFP microscopy

GFP tagged strains were grown and prepared for microscopy similarly as in *section 2.03*. Brightfield (0.006s exposure time, 100% gain) and GFP fluorescence using FITC filters (8s exposure time, 100% gain) were taken across multiple fields of view on the 63X oil-immersion objective. Quantification of abundance was performed by using the total corrected cell fluorescence (TCCF) method as described by McCloy *et al.* (2014)[114].

2.9 RNA sequencing

New England Biolabs rRNA-depleted (Yeast RiboZero) stranded library preparation and RNA sequencing using the Illumina NovaSeq6000 S2 PE100 were conducted by the Genome Quebec Sequencing Centre at McGill University. Reads were aligned to the *Saccharomyces cerevisiae* genome assembly R64-1-1 using STAR[115] and differential expression analysis was performed using DESeq2[116] by the Canadian Centre for Computational Genomics (C3G), a node of the Canadian Genomic Innovation Network supported by the Canadian government through Genome Canada. Transcripts with a FDR adjusted p-value ≤ 0.01 were considered to be

differentially expressed. In brief, reads were trimmed using Trimmomatic[117] from the 3'-end and filtered by setting a phred score cut-off of at least 30 and also have a length of at least 32 bp. Estimated transcript abundances via the metric fragments per kilobase of exon per million fragments mapped (FPKM) was performed using Cufflinks[118]. Gene ontology analysis was done using DAVIDv6.8[119].

2.10 Genome-wide chemogenomics screen

The *Saccharomyces cerevisiae* MATa yeast deletion mutant array (~4200 strains) was arrayed in duplicate on YPD agar (condensed to 1536 colonies per plate) supplemented with G418 using a Singer RoTor HDA (Singer Instruments). Using these condensed plates, colonies were pinned onto triplicate YP and YPM agar plates and incubated for 30°C. The number of days for incubation depended on when each condensed plate had the lowest difference in average colony size between media, leading to a range of 2-4 days. Images were taken using the Bio-Rad Chemidoc™ XRS system under EPI-white light illumination and growth was assessed using SGAtools as described by Wagih *et al.* (2013)[120]. Colonies were aligned to gene names via R ver1.1.453 software. Average growth scores on each medium were assessed by comparing strain growth on YPM to YP, and calculated ratios for every strain were ranked on whether they demonstrated improved growth on mucin (ie. positive impact, larger colonies) or decreased growth on mucin (ie. negative impact, smaller colonies). This was done through two different approaches: 1) by comparing average colony size of each strain from YPM to YP, and 2) by comparing each pinned colony of each strain from YPM to YP. Combining the top 30 strains from the positive impact group (Supplemental Table S4) and negative impact group (Supplemental Table S5) by using each approach, these hits were confirmed by conducting dot assays on YPD, YP and YPM

(Supplemental Figure S5). Strains were subsequently categorized into three groups: 1) YPM > YP, 2) YPM = YP (but growth was less than WT strain on YPM), and 3) YPM < YP.

2.11 Mitochondrial morphology and abundance

Cit1-RFP strains were grown overnight at 30°C in YPD medium. Cultures were then re-inoculated into 50 mL of YP, YPM and YPD to an OD600 of 0.1 and incubated at 30°C. After one day, 5 mL of culture was harvested and cells were resuspended in SC media for brightfield (0.006 sec exposure time, 100% gain) and red fluorescence (0.5 sec, 100% gain) for mitochondrial morphology using the FITC filters portion of the Leica setup (*see section 2.03*). Z-stacked images taken at 0.2 uM steps for a total of 30 planes were taken at multiple fields of view in order to capture at least 50 cells per sample on the 63X oil-immersion objective. Mitochondrial (ie. Cit1-RFP) abundance was quantified using the TCCF method[114], normalized to WT cell fluorescence in the same medium.

2.12 Seahorse assay

Strains were grown overnight at 30°C in YPD. Cultures were then washed in YP, re-inoculated into 120 mL of YP and YPM to an OD600 of 0.1 and incubated at 30°C for one day. To make 2% ethanol supplemented YP (YPE) cultures, overnight strains were re-inoculated into 50 mL of YPE to an OD600 of 0.1 and incubated for six hours. Poly-L-lysine (Sigma, CAT#25988-63-0) was added to the Agilent Seahorse XF96 plates (CAT#101085-004) by pipetting 30 uL of 0.1 mg/mL into each well and incubating on a rocking platform for five minutes. Plates were allowed to dry for two hours prior to experiment. Sensor cartridges for the Seahorse assay were

incubated with calibrant at 37°C for two hours as well. After incubation, cultures were split into three falcon tubes (40 mL each), and resuspended into minimal media (0.167% YNB, 0.5% ammonium sulfate). Cell counting was performed to determine cell concentration, and cell suspensions were diluted such that each well containing 180 uL of suspension had 5x10^5 cells. The plate contained three technical replicates and six blanks per medium. The plate was centrifuged at 500 rpm for 3 min and incubated at 30°C for 30 min. To stop mitochondrial oxygen consumption during the Seahorse assay, 0.05% sodium azide was added as described by Srikumar *et al.* (2013)[121]. Oxygen consumption rate was measured before and after the addition of sodium azide on the Agilent Seahorse XFe96 system. Two-tailed unpaired t-test was performed for each deletion mutant against the WT strain for statistical significance with the GraphPad Prism software.

2.13 Statistical Analysis

To assess statistical significance, two-tailed unpaired t-tests were performed since all analyses involved comparing two independent groups. Tests and standard deviations were calculated for at least three experimental replicates using the GraphPad Prism 8 software (GraphPad Software Inc., La Jolla, California).

3.0 Results

3.1 *S. cerevisiae* can utilize mucin as a carbon source but reduces cell size

As it is currently unknown whether *S. cerevisiae* can grow in the presence of mucin, my initial objective was to assess the growth and morphology of S288C wild type (WT) BY4743 yeast on solid and liquid media with 0.5% mucin (Figure 3A). This concentration of mucin was chosen due to previous work conducted on *C. albicans*[49], and takes into consideration the difficulty of creating high concentrations of a mucin working solution. This work showed that *S. cerevisiae* growth is not hindered by mucin on agar plates (YPM) and may have improved growth over agar with no major carbon source (YP) (Figure 3B). Similarly, *S. cerevisiae* had significantly better growth in liquid YPM compared to cells grown in YP alone (Figure 3C). Subsequently, when mucin adapted yeast (2nd generation – frozen) were cultured in YPD and re-inoculated in YPM, cells displayed no significant difference in growth and doubling time to 1st generation YPM cells (Supplemental Figure S1C and S1D). Furthermore, *S. cerevisiae* cells remain their characteristic round shape in YPM (Figure 3D) but were significantly smaller than cells grown in YPD and YP (1.8-fold and 1.4-fold, respectively) (Figure 3E). Similar to the growth curve analyses, when 1st generation YPM cells were re-inoculated into YPD and YP, they reverted back to a normal size. Taken together, this work suggests that S288C yeast cells are remodelling their metabolism and morphology to utilize mucin and that the improved growth on mucin is not a reflection of acquired mutations.

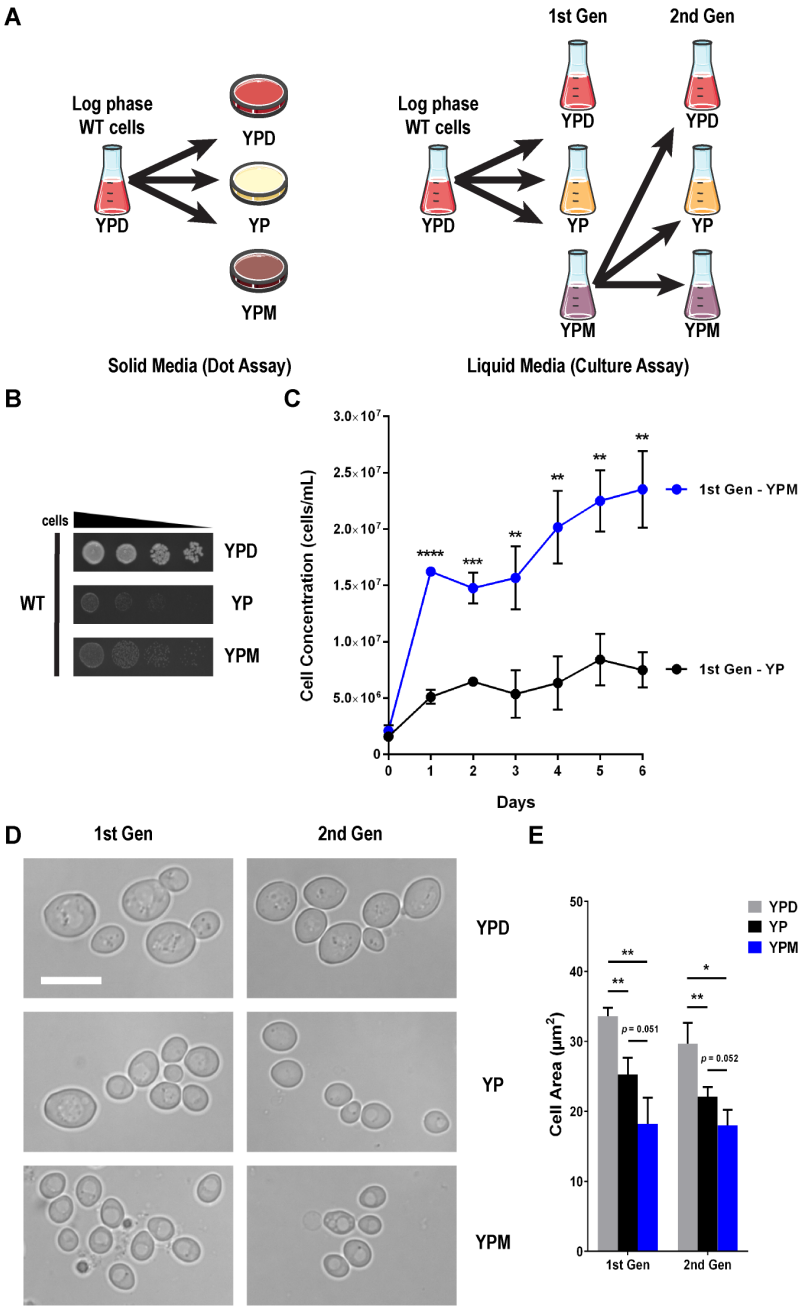

Figure 3 *S. cerevisiae* can metabolize mucin as a carbon source but reduces cell size. (A) Flow diagram of yeast growth in solid and liquid mucin media. (B) Mucin did not hinder growth on solid media. WT (YKB1117) cells were grown to mid log phase in YPD, washed in YP and diluted to a final OD600 of 0.2. Four 10-fold serial dilutions were spotted onto YPD, YP and YPM agar plates. Plates were incubated for two days at 30°C and are representative of three biological replicates. (C) *S. cerevisiae* grew in mucin liquid media. WT cells were grown to mid log phase in YPD, washed in YP and reinoculated into 50 mL of YP (black) and YPM (blue) media (1st Gen). Cultures were incubated for six days at 30°C and cell concentration was measured via cell counting on a hemocytometer by aliquoting 100 uL of culture every 24 hrs. (D) Live-cell images of *S. cerevisiae* grown in different media. WT cells were grown to mid log phase in YPD, washed in YP and reinoculated into 50 mL of YPD, YP and YPM media. 1st generation cells were incubated for 24 hrs, at which time 5 mL of each culture was aliquoted for cell harvest. Cell pellets were resuspended in SC medium prior to brightfield imaging. After six days, cells were harvested, washed in YP and reinoculated into new YPD, YP and YPM media. 2nd generation cells were incubated, aliquoted and imaged similarly. Scale bar represents 10 μm. (E) Quantification of 1st and 2nd generation cell areas for three biological replicates in YPD (grey), YP (black) and YPM (blue) media. All error bars denote standard deviation (SD). * - $p \leq 0.05$, ** - $p \leq 0.01$, *** - $p \leq 0.001$, **** - $p \leq 0.0001$.

3.2 The aspartyl protease Yps7 is important for *S. cerevisiae* growth on mucin

C. albicans possesses secreted aspartyl proteases (SAPs) that can break down mucin in growth media[82], but it is presently not known if *S. cerevisiae* has similar proteins. I used the NCBI Basic Local Alignment Search Tool (BLAST) and identified two protein homologues to *C. albicans'* SAPs found in *S. cerevisiae*, Yps1 and Yps3. These Yapsin (Yps) proteins are part of a family of six aspartyl proteases that also include Yps2, Yps5, Yps6 and Yps7, many of which remain uncharacterized. As Sap2 activity is induced upon mucin exposure[82], I first asked if any *YPS* genes are induced in mucin medium. Through qRT-PCR, both *YPS3* and *YPS7* were significantly induced 1.6-fold and 4-fold in YPM, respectively (Figure 4A). In parallel, I assessed the importance of individual Yps proteins for growth on mucin by conducting dot assays on YPD and YPM using knockout mutants for each of the six *YPS* genes found in *S. cerevisiae* (Figure 4B). While the majority of deletion mutants had no drastic impact on growth when compared to the WT, ***yps7*Δ** displayed the most growth deficiency on YPM compared to the WT.

As Yapsin family members could be functionally redundant, I constructed double and triple knockout mutants with genes that had either high similarity to *C. albicans'* SAPs (*yps1*Δ, *yps3*Δ) or promising dot assay results (*yps7*Δ) and assessed growth on mucin media. While the *yps1*Δ*yps7*Δ and *yps3*Δ*yps7*Δ displayed mild growth defects similar to *yps7*Δ, the triple knockout mutant (*yps1*Δ*yps3*Δ*yps7*Δ) had reduced growth on YPD and a severe growth defect on YPM (Figure 4C). This suggests that Yps1, Yps3 and Yps7 are functionally redundant for a yet to be identified biological function. The upregulation of *YPS7* mRNA and the observable growth defect of *yps7*Δ cells on mucin suggest that Yps7 is important for *S. cerevisiae* growth on mucin media, and in its absence Yps1 and Yps3 can partially grow on mucin.

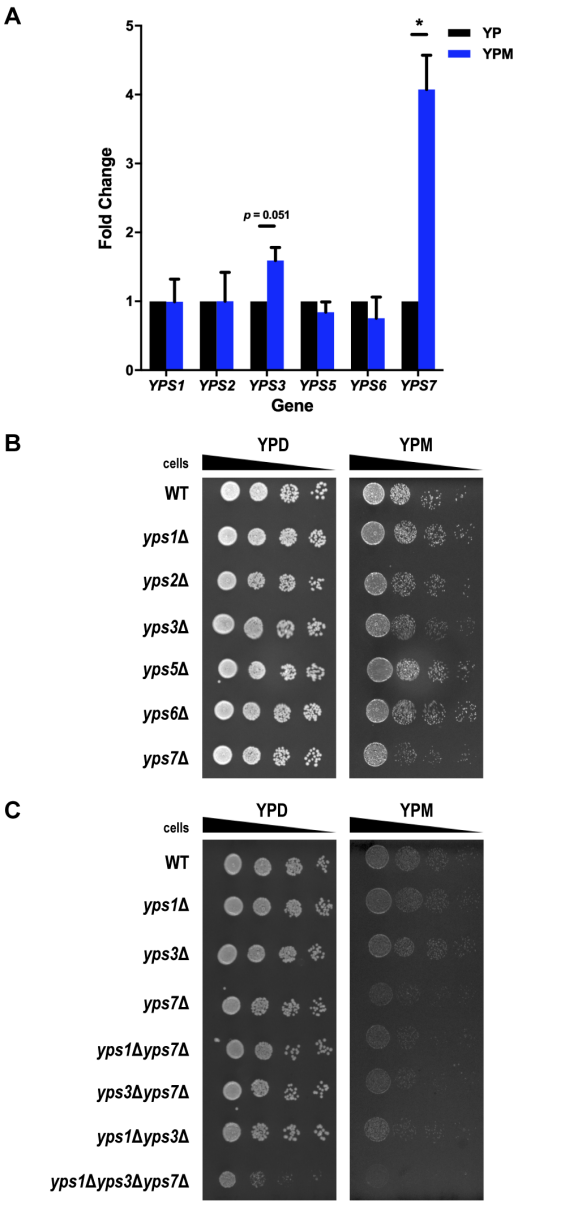

Figure 4 *YPS7* gene expression is induced upon mucin exposure and *yps7*Δ cells display reduced growth on mucin. (A) WT (YKB1117) cells were grown to mid log phase in YPD, washed in YP and reinoculated into 50 mL of YP (black) and YPM (blue) media. Cultures were incubated for 24 hrs at 30°C prior to cell harvest and normalized to the lowest concentrated culture. Cells were then lysed via beadbeating and RNA was extracted via the phenol:chloroform:isoamyl alcohol method. RNA concentration and integrity was assessed via nanodrop and gel electrophoresis. qPCR was conducted using EvaGreen and fold changes were analyzed with the **ΔΔ**CT method normalized to YP levels. All error bars denote SD, * - $p \leq 0.05$. (B) WT (YKB1079), along with *yps1*Δ (YKB4828), *yps2*Δ (YKB5015), *yps3*Δ (YKB4829), *yps5*Δ (YKB4830), *yps6*Δ (YKB4832) and *yps7*Δ (YKB4831) strains were grown to mid log phase in YPD, washed in YP and diluted to a final OD600 of 0.2. Four 10-fold serial dilutions were spotted onto YPD and YPM agar plates. (C) WT (YKB1079), along with *yps1*Δ, *yps3*Δ, *yps7*Δ, *yps1*Δ*yps7*Δ (YKB4897), *yps3*Δ*yps7*Δ (YKB4898), *yps1*Δ*yps3*Δ (YKB4899) and *yps1*Δ*yps3*Δ*yps7*Δ (YKB4900) strains were grown to mid log phase in YPD, washed in YP and diluted to a final OD600 of 0.2. Four 10-fold serial dilutions were spotted onto YPD and YPM agar plates. All plates were incubated for two days at 30°C and are representative of three biological replicates.

3.3 Yps7 displays differences in subcellular localization in mucin medium compared to YPD and YP

As the genetics suggests Yps1, Yps3 and Yps7 may have functional redundant roles for growth on mucin, I next assessed their subcellular localization and abundance. Their subcellular localizations were assessed in YPD, YP and YPM using C-terminal tagged GFP-strains for each Yps protein. Similar to what was previously reported in YPD[122], Yps1-GFP displayed diffuse cytoplasmic staining, while Yps3-GFP displayed diffuse staining along with potential enrichment of a subfraction at the mitochondria (Figure 5A). Additionally, incubation in YP or YPM did not change the localization of Yps1-GFP and Yps3-GFP, though there may be a reduction of Yps3-GFP at the mitochondria, which would require further exploration. In contrast, Yps7-GFP appears compartmentalized in YPD and YP, likely at the vacuole as predicted for other Yps proteins in high-throughput studies[123]. Upon incubation in YPM, Yps7-GFP signal becomes more diffuse across the cytoplasm. By quantifying GFP fluorescence, I determined that Yps7-GFP was significantly increased in YPM compared to YPD (Figure 5B). This provides further evidence that Yps7 may have a distinct role for growth in mucin conditions.

3.4 Mucin induces cellular stress but *yps7*Δ growth deficiency is not rescued after alleviating osmotic or cell wall stresses

Yps proteins have been shown to be involved in MAPK signalling through the activation of Msb2[72]. These include pathways that induce filamentous growth, pheromone response and the HOG pathway[124]. Due to the density of mucin glycoproteins in the medium, it is also possible that osmotic stress could be a potential factor for the reduction in growth upon deletion of *YPS7*. To

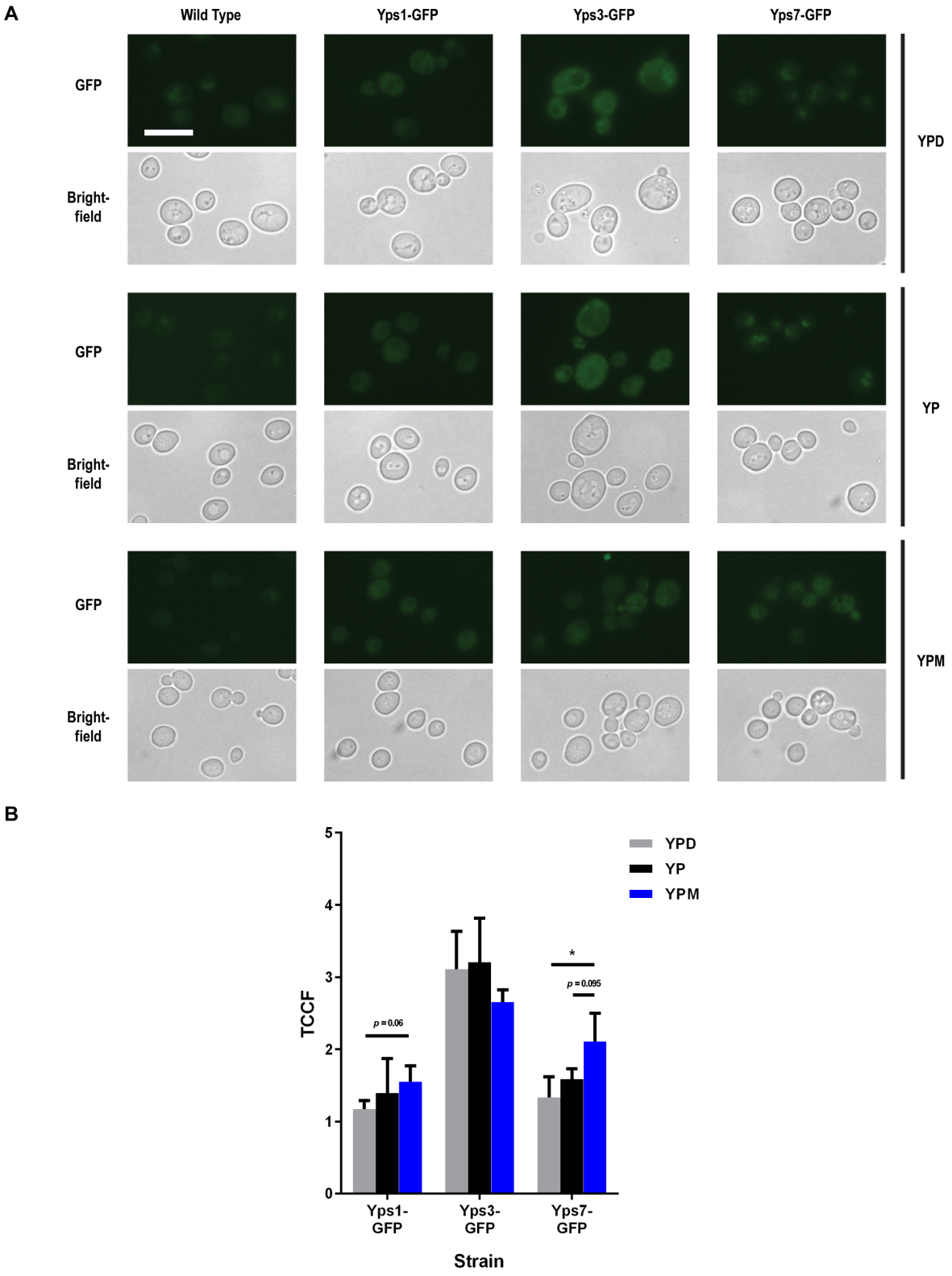

Figure 5 Yapsin proteins were diffused throughout the cell in YPM and only Yps7 is induced in mucin media. (A) WT (YKB1079) and GFP-tagged Yps1 (YKB4901), Yps3 (YKB4902) and Yps7 (YKB4903) strains were grown to mid log phase in YPD, washed in YP and reinoculated into 50 mL of YPD, YP and YPM media. Cultures were incubated for 24 hrs, at which time 5 mL of each culture was aliquoted for cell harvest. Cell pellets were resuspended in SC medium prior to GFP and brightfield imaging. Scale bar represents 10 µm. (B) Quantification of GFP by total corrected cell fluorescence (TCCF) for three biological replicates in each media. All error bars denote SD. * - $p \leq 0.05$.

assess this, I transformed single (*yps7*Δ), double (*yps1*Δ*yps7*Δ, *yps3*Δ*yps7*Δ) and triple (*yps1*Δ*yps3*Δ*yps7*Δ) knockout mutants with the high copy p5476 overexpression plasmid for *HOG1*, which is the primary activator of the hyperosmotic stress response[73], and conducted dot assays on SD medium with dextrose (SD-Leu; control), SD-Leu + 1 M NaCl (osmotic stress) and mucin (SM-Leu). As expected, growth deficiency in *hog1*Δ in the presence of 1 M NaCl was rescued after exogenous expression of *HOG1* (Figure 6A). However, there was no growth deficiency observed for any *yps7*Δ strains on NaCl medium. Further, there was no growth deficiency observed in *hog1*Δ grown on mucin medium. There does appear to be a weak hyperosmotic sensitivity observed in the *yps1*Δ*yps3*Δ*yps7*Δ when grown in NaCl, however overexpression of *HOG1* did not rescue any growth deficiencies in the *yps7*Δ strains on YPM. This indicates that the Yps proteins tested are not required to buffer osmotic stress and that growth on mucin does not require the HOG pathway.

Although there is little information known about the biological function of Yps7, previous research suggests it may be involved in cell wall integrity[89,125]. Therefore, I next asked whether mucin has an impact on cell wall integrity via Yps7. I assessed the growth of *yps7*Δ, *yps1*Δ*yps7*Δ, *yps3*Δ*yps7*Δ and *yps1*Δ*yps3*Δ*yps7*Δ on YPM grown at 37°C with and without the addition of 1 M sorbitol. Sorbitol is a known osmotic stabilizer and is often added to the media at elevated temperatures in order to rescue the growth deficiency of knockout mutants with defects in cell wall integrity[124,126]. Slt2 is a mitogen-activated protein kinase that regulates cell wall integrity and its deletion is commonly used as a control for sorbitol rescue during growth at 37°C[127]. As expected, *slt2*Δ displayed mild but reproducible growth defects at 37°C on YPD (Figure 6B). In contrast, *slt2*Δ could not grow on mucin at 37°C, suggesting that mucin treatment is affecting cell wall integrity since addition of sorbitol rescues its growth defect on mucin medium. In addition, while at 30°C there was no observable genetic interaction, *yps1*Δ*yps7*Δ displayed a mild growth defect

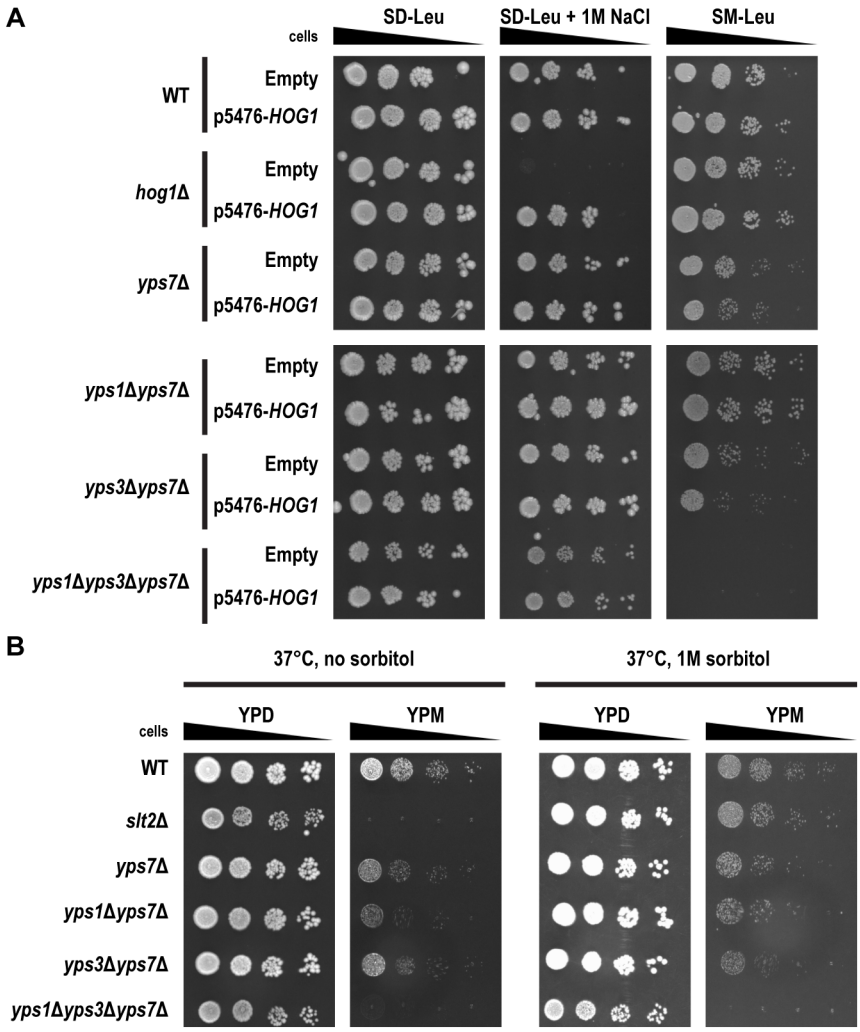

Figure 6 Mucin induces cellular stress, but *yps7*Δ growth deficiency is not rescued after alleviating osmotic or cell wall stresses. (A) WT (YKB1079), *hog1*Δ (YKB4919), *yps7*Δ (YKB4831), *yps1*Δ*yps7*Δ (YKB4897), *yps3*Δ*yps7*Δ (YKB4898) and *yps1*Δ*yps3*Δ*yps7*Δ (YKB4900) strains that were transformed with the high copy p5476 overexpression plasmid for *HOG1* were grown to mid log phase in YPD, washed in SD medium and diluted to a final OD600 of 0.2. Four 10-fold serial dilutions were spotted onto SD-Leu, SD-Leu + 1M NaCl and SM-Leu agar plates. Plates were incubated for six days at 30°C and are representative of three biological replicates. (B) WT (YKB1079), along with *slt2*Δ (YKB4917), *yps7*Δ, *yps1*Δ *yps7*Δ, *yps3*Δ*yps7*Δ and *yps1*Δ*yps3*Δ*yps7*Δ were grown to mid log phase in YPD, washed in YP and diluted to a final OD600 of 0.2. Four 10-fold serial dilutions were spotted onto YPD and YPM agar plates, with or without the addition of 1M sorbitol. Plates were incubated for three days at 37°C and are representative of three biological replicates.

at 37°C on mucin medium. While sorbitol could rescue the growth defects of *yps1*Δ*yps7*Δ, no rescue was observed for the growth defects of *yps1*Δ*yps3*Δ*yps7*Δ at 37°C on mucin medium. Therefore, although the growth defects of *yps7*Δ strains in mucin are not entirely due to cell wall processes, mucin does seem to produce a cell wall stress that may involve one of the Yps proteins (Yps1).

3.5 RNA-sequencing demonstrates drastic transcriptome remodelling during growth in mucin and the importance of mitochondrial-associated genes

To take a more global approach, I compared the transcriptomes of *S. cerevisiae* growth in the absence or presence of mucin. RNA samples were extracted from cells cultured in YP and YPM for one day at 30°C, and subsequently analyzed via Illumina sequencing. Each sample had >90% read alignment to the *S. cerevisiae* genome assembly R64-1-1, accounting for approximately 5000 genes. Principal component analysis demonstrated clustering of sample replicates and variance can be mainly attributed to sample group (Supplemental Figure S4A). In total, 2131 genes showed significant differential expression comparing cells grown in YPM to cells grown in YP with an FDR adjusted p-value ≤ 0.01 (Supplementary Figure S4B). This includes all significantly differentially expressed genes, with no fold change cut-off. These parameters were chosen in order to include a known control for gene regulation in mucin conditions, which was Yps7. Yps7 was upregulated 1.5-fold based on sequencing (data not shown).

To determine pathways regulated by *S. cerevisiae* during growth in mucin, I assessed the top 50 upregulated (Table 1) and downregulated (Table 2) genes for gene ontology (GO) analyses using DAVIDv6.8[119]. Among the upregulated genes, there was an enrichment for gene products involved in mitochondrial function including ATP synthase biogenesis ($p = 0.00273$) (*ATP22*,

Table 1 – Top 50 upregulated genes in YPM compared to YP ranked by fold change.

Rank	Systematic Name	Gene Name	Fold Change	P-Value	FDR
1	YJR068W	RFC2	15.89	1.30e-09	9.74e-07
2	YPL270W	MDL2	15.12	1.09e-07	7.74e-06
3	YHL026C	YHL026C	14.88	3.78e-08	4.06e-06
4	YPL160W	CDC60	13.06	6.26e-07	2.35e-05
5	YPL283C	YRF1-7	11.19	1.32e-05	1.64e-04
6	YNL071W	LAT1	9.43	2.41e-06	5.53e-05
7	YDR278C	YDR278C	9.20	7.06e-04	3.02e-03
8	tQ(CUG)M	CDC65	6.40	1.73e-05	1.96e-04
9	YLR315W	NKP2	5.89	9.31e-06	1.32e-04
10	YDR350C	ATP22	5.78	5.73e-08	5.44e-06
11	YPR091C	NVJ2	5.56	5.31e-05	4.23e-04
12	YDR203W	YDR203W	5.56	2.26e-05	2.34e-04
13	YPL200W	CSM4	5.53	7.04e-09	1.97e-06
14	YER168C	CCA1	5.42	9.13e-07	2.98e-05
15	YLR133W	CKI1	5.35	1.09e-07	7.74e-06
16	YDR492W	IZH1	5.26	1.45e-06	3.91e-05
17	YDL118W	YDL118W	5.19	3.04e-06	6.46e-05
18	YOR343C	YOR343C	5.08	3.21e-10	4.50e-07
19	YDR014W-A	HED1	4.86	1.63e-08	3.29e-06
20	YGL171W	ROK1	4.49	2.05e-05	2.18e-04
21	YNR020C	ATP23	4.46	9.13e-08	6.90e-06
22	YDL237W	AIM6	4.45	7.27e-05	5.27e-04
23	YHL007C	STE20	4.31	2.29e-07	1.23e-05
24	YKL187C	FAT3	4.21	1.33e-07	8.86e-06
25	YJR072C	NPA3	4.20	5.28e-07	2.11e-05
26	YDR301W	CFT1	4.18	1.99e-07	1.12e-05
27	YER154W	OXA1	4.12	9.84e-07	3.06e-05
28	YLR203C	MSS51	4.11	2.35e-08	3.60e-06
29	YFR042W	KEG1	4.10	2.35e-06	5.42e-05
30	YPL161C	BEM4	4.05	4.37e-06	8.32e-05
31	YPR143W	RRP15	4.04	7.61e-06	1.17e-04
32	YFR041C	ERJ5	3.98	9.55e-08	7.06e-06
33	YLR397C	AFG2	3.89	2.25e-08	3.60e-06
34	YDR320W-B	YDR320W-B	3.78	1.38e-06	3.81e-05
35	YBR260C	RGD1	3.70	2.70e-05	2.68e-04
36	YIL065C	FIS1	3.68	3.48e-05	3.17e-04
37	YIL021W	RPB3	3.67	3.11e-04	1.59e-03
38	YHR150W	PEX28	3.65	6.30e-06	1.03e-04
39	YOR268C	YOR268C	3.63	2.69e-09	1.13e-06
40	YJR094W-A	RPL43B	3.60	4.54e-06	8.52e-05
41	YGL066W	SGF73	3.58	1.11e-05	1.49e-04
42	YOL099C	YOL099C	3.58	4.83e-04	2.24e-03
43	YLR190W	MMR1	3.57	3.46e-08	4.01e-06
44	YNL312W	RFA2	3.55	6.50e-06	1.05e-04
45	YLR447C	VMA6	3.53	4.19e-09	1.57e-06
46	YMR138W	CIN4	3.52	6.06e-06	1.00e-04
47	YER055C	HIS1	3.51	2.30e-03	7.73e-03
48	YKR023W	RQT4	3.44	1.40e-05	1.71e-04
49	YLR191W	PEX13	3.44	1.86e-07	1.08e-05
50	YOR245C	DGA1	3.41	5.54e-06	9.64e-05

Table 2 – Top 50 downregulated genes in YPM compared to YP ranked by fold change.

Rank	Systematic Name	Gene Name	Fold Change	P-Value	FDR
1	YPL227C	ALG5	-21.47	1.05e-09	8.80e-07
2	YOR372C	NDD1	-15.73	3.84e-11	1.29e-07
3	YNL273W	TOF1	-14.46	3.52e-11	1.29e-07
4	YNL047C	SLM2	-13.73	4.19e-10	4.50e-07
5	YHR214W	YHR214W	-13.05	3.78e-08	4.06e-06
6	YLR164W	SHH4	-11.85	2.18e-08	3.60e-06
7	YGL248W	PDE1	-11.37	4.32e-04	2.05e-03
8	YBR056W-A	MNC1	-10.78	2.93e-10	4.50e-07
9	YHR107C	CDC12	-9.66	3.37e-10	4.50e-07
10	YHR206W	SKN7	-9.47	1.36e-08	3.25e-06
11	YLR385C	SWC7	-9.31	1.97e-09	1.02e-06
12	tE(UUC)Q	tE(UUC)Q	-8.53	1.91e-09	1.02e-06
13	YMR155W	YMR155W	-8.21	1.73e-07	1.04e-05
14	snR18	snR18	-8.02	2.18e-08	3.60e-06
15	YJR105W	ADO1	-7.96	2.92e-07	1.45e-05
16	YBR131W	CCZ1	-7.94	7.46e-08	6.12e-06
17	YGL253W	HXK2	-7.89	6.13e-07	2.33e-05
18	YGR033C	TIM21	-7.88	7.36e-07	2.64e-05
19	YAR020C	PAU7	-7.80	2.65e-05	2.65e-04
20	YNR018W	RCF2	-7.79	1.80e-07	1.05e-05
21	YIL051C	MMF1	-7.59	3.62e-06	7.28e-05
22	YOR079C	ATX2	-7.46	3.75e-05	3.33e-04
23	YFL060C	SNO3	-7.45	1.61e-09	1.02e-06
24	YLR294C	YLR294C	-7.32	1.43e-07	9.25e-06
25	YDL097C	RPN6	-7.19	5.34e-07	2.12e-05
26	YMR288W	HSH155	-6.99	2.11e-09	1.02e-06
27	YHR020W	YHR020W	-6.72	1.92e-08	3.60e-06
28	YLR434C	YLR434C	-6.53	2.69e-09	1.13e-06
29	YPL233W	NSL1	-6.50	7.22e-06	1.13e-04
30	YGL169W	SUA5	-6.36	5.78e-08	5.44e-06
31	YML070W	DAK1	-6.34	1.14e-04	7.44e-04
32	YMR238W	DFG5	-6.30	7.40e-06	1.15e-04
33	YML057W	CMP2	-6.30	1.58e-05	1.86e-04
34	YLR086W	SMC4	-6.29	4.68e-10	4.50e-07
35	YMR006C	PLB2	-6.07	2.44e-08	3.60e-06
36	YHR031C	RRM3	-6.04	4.61e-04	2.16e-03
37	YGL068W	MNP1	-6.03	1.50e-08	3.25e-06
38	YGR224W	AZR1	-5.94	3.31e-08	3.97e-06
39	YKL122C	SRP21	-5.80	1.62e-07	1.00e-05
40	YMR218C	TRS130	-5.70	3.03e-08	3.71e-06
41	YKL193C	SDS22	-5.65	9.38e-09	2.52e-06
42	YNR042W	YNR042W	-5.56	7.91e-06	1.20e-04
43	YOL155C	HPF1	-5.52	6.58e-08	5.70e-06
44	YIL151C	ESL1	-5.48	3.39e-05	3.14e-04
45	YGL174W	BUD13	-5.32	1.32e-04	8.36e-04
46	tE(UUC)M	tE(UUC)M	-5.26	2.42e-08	3.60e-06
47	YKL150W	MCR1	-5.22	1.20e-07	8.20e-06
48	YHR214W-A	YHR214W-A	-5.19	8.85e-05	6.10e-04
49	YBR146W	MRPS9	-5.15	5.18e-09	1.83e-06
50	YFR019W	FAB1	-5.11	1.36e-06	3.78e-05

ATP23, *OXA1*) and positive regulation of mitochondrion organization ($p = 0.00837$) (*ATP22*, *FIS1*, *MSS51*) (Figure 7A). Another GO category enriched for was organelle fission ($p = 0.0363$) (*CSM4*, *FIS1*, *HED1*, *NKP2*, *NPA3*, *RFA2*, *STE20*), a common feature of the mitochondrion. Among the downregulated genes, there was an enrichment for gene products involved in the mitotic cell cycle process ($p = 0.0504$) (*BUD13*, *CDC12*, *NDD1*, *NSL1*, *SDS22*, *SMC4*, *TOF1*) and cell division ($p = 0.0541$) (*BUD13*, *CDC12*, *DFG5*, *NSL1*, *SDS22*, *SMC4*) (Figure 7B). Overall, this suggests that cells require mitochondrial function to metabolize mucin and that progression through the cell cycle is potentially affected in mucin.

3.6 Chemogenomics screen showcases various essential biological processes during growth on mucin and highlights the importance of mitochondrial function

To complement the transcriptome analysis, I screened the *Saccharomyces cerevisiae* Deletion Mutant Array[108] for genes that when deleted modulate growth on mucin (Figure 8A). The deletion mutant collection was first screened on both YP and YPM, and any mutants that displayed differential growth were confirmed by dot assay. The screen identified 30 genes that when deleted resulted in improved growth (YP growth < YPM growth, 19 genes), decreased growth (YP growth > YPM growth, 2 genes) or had no impact on their growth but were growth deficient compared to the WT (YP growth = YPM growth, 9 genes) on YPM compared to their growth on YP (Figure 8B). There were no deletion mutants that showed improved growth on YPM compared to the WT. However, despite showing improved growth on YPM compared to their growth on YP, there were five genes that showed similar growth to the WT on YPM upon their deletion (*MDM35, MRS2, PEX19, VPS15, YIM2*).

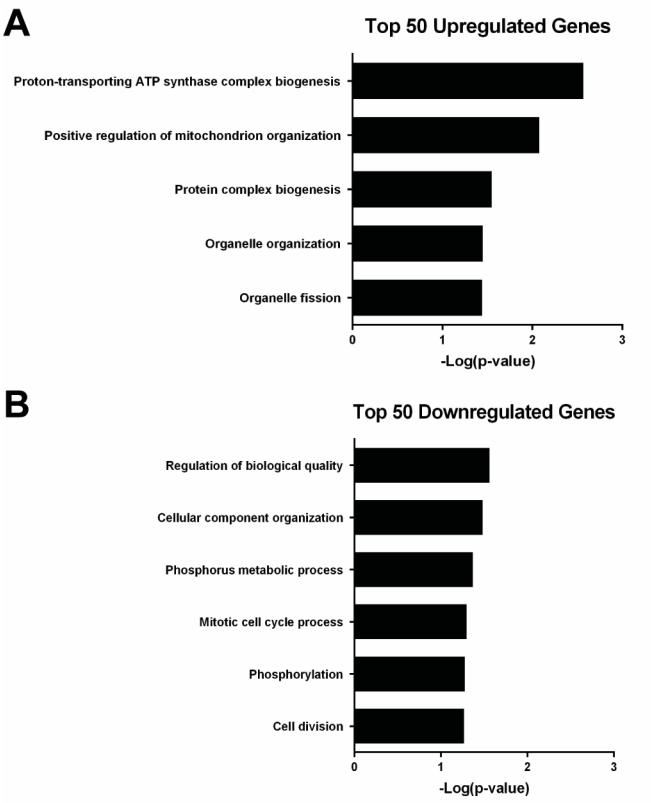

Figure 7 Gene ontology analysis for upregulated and downregulated genes are enriched for gene products involved in mitochondrial function and the cell cycle. (A) Functional enrichment for top 50 upregulated genes in YPM compared to YP. (B) Functional enrichment for top 50 downregulated genes in YPM compared to YP. Genes were organized based on biological process using DAVIDv6.8 and plotted with a threshold p-value of ≤ 0.05.

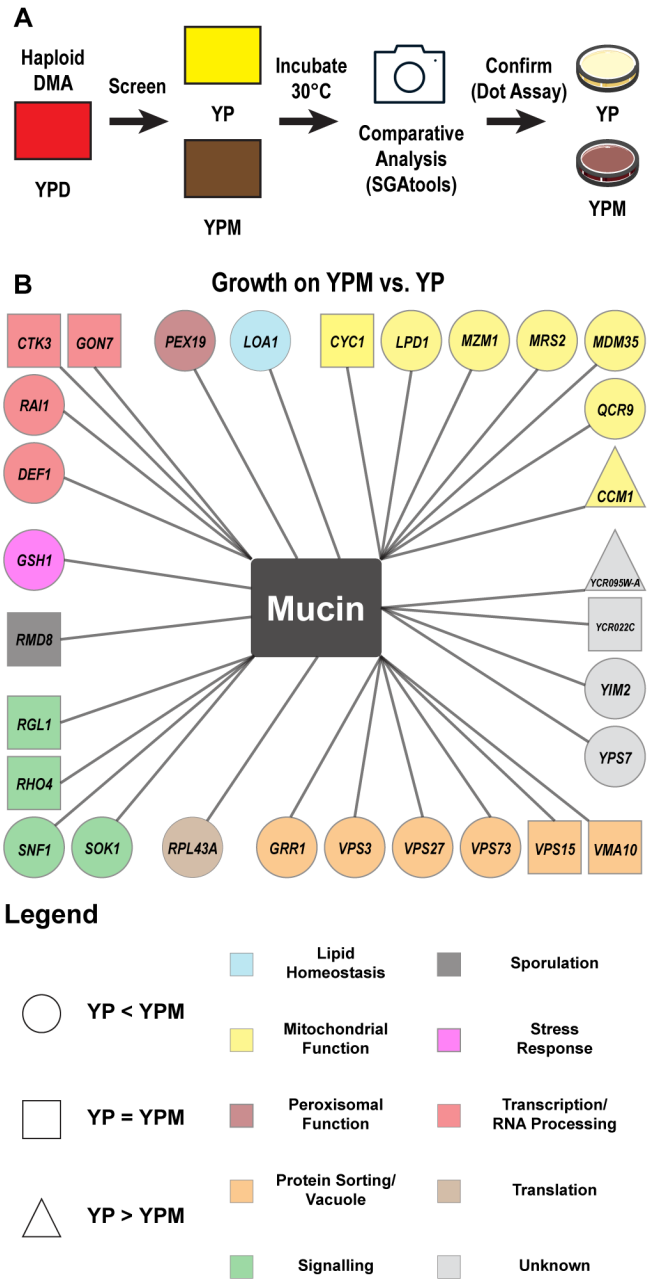

Figure 8 Distinct chemogenomic profile for *S. cerevisiae* growth on mucin comparing to growth on YP. (A) Flow diagram of mucin screen. Comparative analysis was conducted using growth scores obtained via SGAtools for each strain on YP and YPM. YPM/YP score ratios obtained for each strain were calculated and ranked. Confirmation was conducted for the highest (postive impact deletion) and lowest (negative impact deletion) ratios by comparing growth via dot assays. (B) Deletion mutants identified in the screen have been colour coded based on biological process. Shapes indicate whether gene deletion resulted in a positive impact (grew better on YPM than on YP, O), negative impact (grew worse on YPM than on YP, Δ) or no change (grew equally on YPM and on YP but growth deficient compared to the WT on YPM, □) based on confirmational dot assays.

Genes identified in the screen were categorized by biological process using their descriptions listed in the *Saccharomyces* Genome Database. Deletion mutants that displayed improved growth on YPM compared to their growth on YP were implicated in mitochondrial function (*LPD1, MDM35, MRS2, MZM1, QCR9*), protein sorting or vacuolar function (*GRR1, VPS3, VPS27, VPS73*), transcription and RNA processing (*DEF1, RAI1*), signalling (*SNF1, SOK1*), among others. Interestingly, *SNF1* is known to be important for *S. cerevisiae* growth in poor carbon conditions and even regulates filamentous morphology[71]. *YPS7* also appeared on this list, as the growth defect is more enhanced in YP compared to YPM. It is possible that Yps7 may be important for overall growth in poor conditions when resources are scarce.

The only two deletion mutants that displayed reduced growth on YPM compared to their growth on YP were *CCM1* and *YCR095W-A*. Ccm1 is a mitochondrial 15S rRNA-binding protein that is involved in the stabilization of *COB* and *COX1* pre-mRNAs, two components of the electron transport chain[128]. Ycr095w-a is a putative protein of unknown function that has low localization signal to mitochondria[129]. This further suggests the importance of mitochondrial function in regards to growth in media with mucin as the main carbon source.

3.7 Mitochondria fission and biogenesis is induced upon deletion of *CCM1* and *YCR095W-A* during growth in mucin

Both the transcriptome and chemical profiling suggest the mitochondria is playing an important role in the ability of *S. cerevisiae* to utilize mucin. The only two strains that were confirmed to grow worse on YPM compared to YP were also implicated in some way to the mitochondria. Hence, I next looked at the impact of mucin on mitochondrial morphology. I assessed mitochondrial morphology of WT, *ccm1*Δ and *ycr095w-a*Δ cells that expressed Cit1-RFP.

CIT1 encodes citrate synthase, the enzyme responsible for the conversion of acetyl coenzyme A (acetyl-CoA) into citrate at the beginning the tricarboxylic acid cycle and is a common mitochondrial marker[130,131]. As expected, the mitochondria in WT cells grown in YPD were tubular and localized around the periphery of the cell, while the mitochondria in WT cells grown under carbon-limiting conditions of YP became shorter, more abundant and distributed throughout the cell (Figure 9A). Interestingly, the mitochondria of cells grown in YPM seem to resemble a state in between YP and YPD mitochondria. Further, there is a clear increase in the abundance of Cit1-RFP upon incubation in YP and YPM (Figure 9B), suggesting an increase in mitochondrial biogenesis and that cells consider mucin medium a carbon-limiting condition. Unsurprisingly, since Ccm1 is required for the stabilization of electron transport chain pre-mRNAs, *ccm1*Δ cells showed reduced mitochondrial content in YPD, while in *ycr095w-a*Δ cells the mitochondria appeared to be similar to WT. Upon incubation in YP and YPM, morphological changes were even more enhanced within *ccm1*Δ and *ycr095w-a*Δ cells (Figure 9A). Additionally, RFP fluorescence was significantly higher in *ccm1*Δ and *ycr095w-a*Δ cells compared to WT cells grown in YPM (Figure 9B). Thus, cells respond to the deletion of *CCM1* or *YCR095W-A* as if further starved of carbon sources and induce mitochondrial fission and biogenesis in mucin conditions.

3.8 Mitochondrial function is disrupted upon deletion of *YCR095W-A* during growth in mucin

The changes in morphology suggest there may be changes in mitochondrial function when grown in mucin conditions. To assess mitochondrial function, I measured the oxygen consumption rate (OCR) of strains grown in the presence of mucin. Strains were grown in minimal media containing either no carbon source (water), a non-fermentable carbon source (ethanol) or mucin, and OCR was measured before and after the addition of 0.05% sodium azide. Sodium azide is used

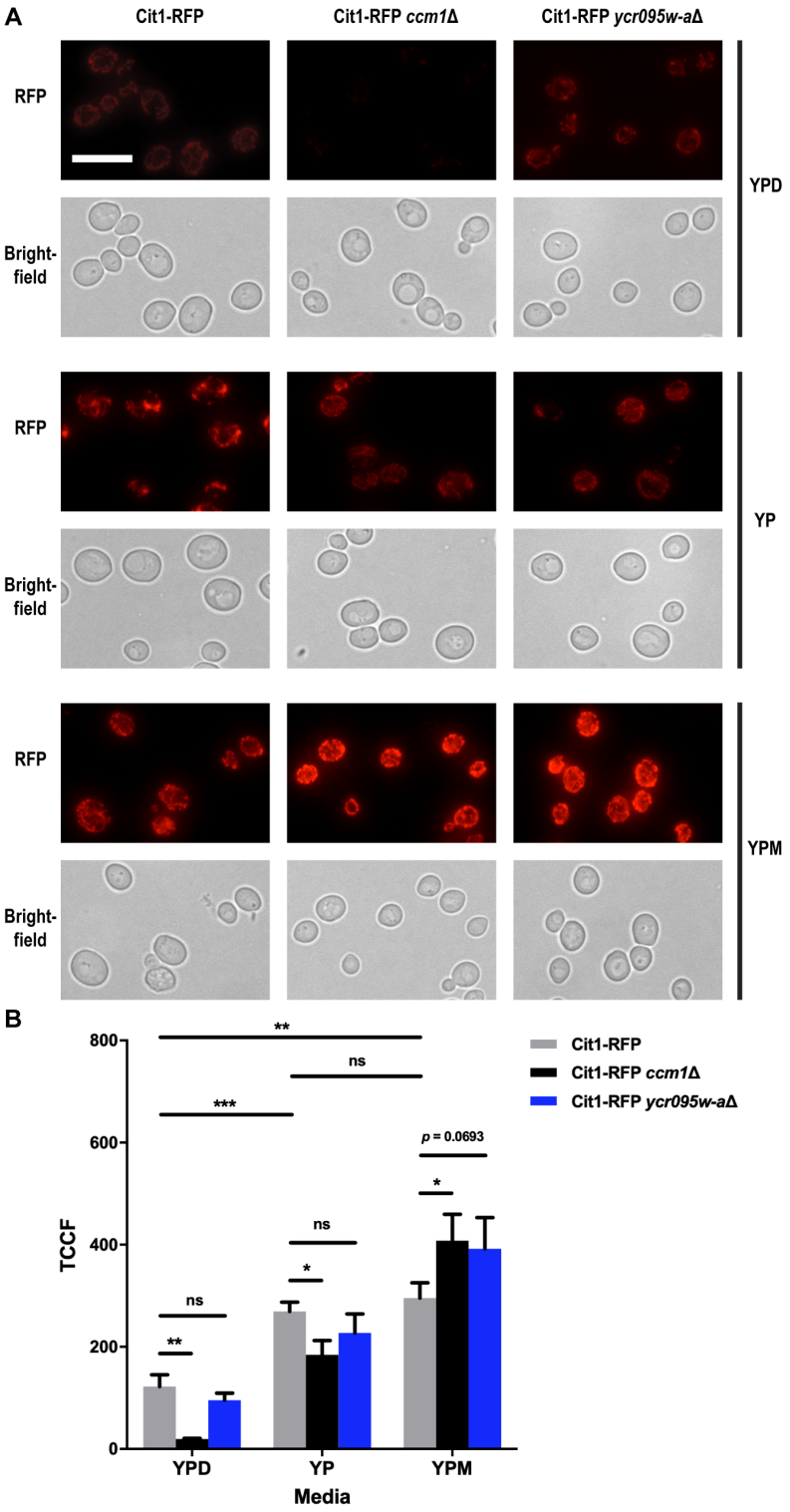

Figure 9 Mucin changes mitochondrial morphology and deletion of *CCM1* or *YCR095W-A* lead to increased Cit1-RFP in mucin media. (A) Cit1-RFP (YKB4907), Cit1-RFP *ccm1*Δ (YKB4942) and Cit1-RFP *ycr095w-aΔ* (YKB4916) were grown to mid log phase in YPD, washed in YP and reinoculated into 50 mL of YPD, YP and YPM media. Cultures were incubated for 24 hrs, at which time 5 mL of each culture was aliquoted for cell harvest. Cell pellets were resuspended in SC medium prior to RFP and brightfield imaging. Scale bar represents 10 µm. (B) Quantification of RFP by total corrected cell fluorescence (TCCF) for three biological replicates in each media. All error bars denote SD. * - $p \leq 0.05$, ** - $p \leq 0.01$, *** - $p \leq 0.001$.

to shut down oxygen consumption from mitochondria by binding and inhibiting the function of cytochrome c oxidase of the electron transport chain[132]. I observed that the OCR of WT cells was significantly higher in the presence of a carbon source, with the highest OCR observed in mucin conditions (Figure 10A). Despite having Cit1-RFP expressed in mitochondria, the OCR of *ccm1*Δ cells was significantly lower in all conditions compared to the WT (Figure 10B). This is not unexpected as null mutants for *CCM1* are known to have dysfunctional mitochondria and therefore have reduced growth on non-fermentable carbon sources[95]. In contrast, the OCR of *ycr095w-a*Δ cells was only significantly lower than WT cells in YPM. This suggests that the product of *YCR095W-A* has a distinct impact on the mitochondria and overall growth when mucin is the main carbon source.

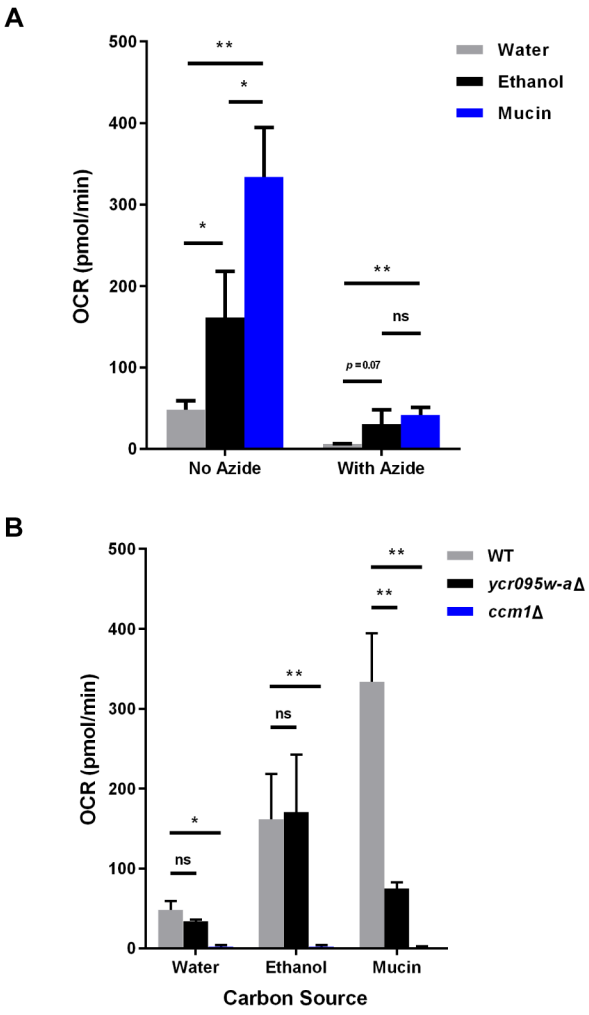

Figure 10 Oxygen consumption rate (OCR) increases in the presence of mucin and disrupted upon deletion of *CCM1* or *YCR095W-A*. (A) WT (YKB1079) cells were grown to mid log phase in YPD, washed in YP and re-inoculated into 50 mL of YP and YPM. Cultures were incubated for 24 hrs, at which time cells were harvested. Cultures for cells grown in ethanol were done on the same day as the Seahorse assay. Cell pellets were resuspended in YNB medium with water, 2% ethanol or 0.05% mucin, and 5x10^5 cells were aliquoted into designated plate wells. OCR was measured via the Agilent Seahorse XFe96 analyzer before and after the addition of 0.05% sodium azide. (B) *ccm1*Δ (YKB4908) and *ycr095w-a*Δ (YKB4912) strains were prepared similarly as above and OCR was also quantified before and after the addition of 0.05% sodium azide. Error bars denote SD. * - $p \leq 0.05$, ** - $p \leq 0.01$.

4.0 Discussion

4.1 Impact of mucin on growth and morphology

Previous research on *C. albicans* has demonstrated its ability to break down mucin as an energy source[49,50,82]. This work showed that by adding a similarly low concentration of mucin to solid or liquid media, cells were able to grow better than in the absence of mucin (Figure 3B and 3C). This suggests that cells were able to metabolize mucin as the main energy source in growth medium. Regarding cell morphology, there was a distinct reduction in growth for cells in mucin compared to cells in glucose (Figure 3D and 3E). This was expected as it is known that poor carbon sources will have smaller critical size requirements before cells progress out of G1 phase[133]. Surprisingly, cells grown in mucin were still smaller than cells grown in medium with no major carbon source at all. Since cell cultures are more concentrated in YPM over YP at any given time, this suggests that progression out of G1 phase occurs faster due to a lower critical size requirement in mucin conditions. These changes provide evidence that the reduction in cell size may be an adaptive response to the specific mucin conditions cells are encountering.

The regulation of genes involved in the cell cycle, which dictates the overall size and morphology of the cell, is heavily dependent on the carbon sources available in the environment[133]. As expected, several genes involved in the progression through mitosis also appeared in the transcriptome data. *NDD1*, encoding an activator of the *CLB2* cluster of genes required for mitosis[134], was drastically downregulated in mucin conditions by 16-fold (Table 2). Additionally, *CDC12*, which encodes the only component of the septin ring that is essential for cytokinesis[135], was downregulated 10-fold (Table 2). Cell size regulators like *SDS22*, whose gene product is involved in chromosome stability and localizes Glc7 to the nucleus in order to activate transcription

of metabolic and physiological processes during cytokinesis[136], was observed to be downregulated 6-fold (Table 2). This is complimented by the fact that regulators for increasing cell size like *SFP1*[137] and *SCH9*[138] were also downregulated in mucin conditions by 1.5-fold and 1.6-fold, respectively (data not shown). These changes provide further evidence that this reduction in cell size may be an adaptive response to the specific mucin conditions cells are encountering. Despite an expected downregulation of mitotic cell division in limited carbon conditions like mucin culture, by reducing critical size requirements, the cell is not arrested in mucin and still progresses through the cell cycle.

4.2 Aspartyl-proteases like Yps7 are important but not involved in potential responses to cell wall integrity or osmotic stress under mucin conditions

In terms of *C. albicans*, previous studies have demonstrated the importance of SAPs in the breakdown of mucin for host penetration and nutrient collection[82,83]. These proteases work best under acidic conditions and are often implicated in the virulence of the opportunistic pathogen in the gut environment[76,77]. This study was the first to compare SAPs to homologues found in *S. cerevisiae* (similar proteases called Yapsins [Yps]), for their role in mucin breakdown. It was shown that *YPS7* mRNA was upregulated 4-fold by the addition of mucin (Figure 4A). *YPS7* was also observed to be upregulated 1.5-fold in mucin conditions through RNA-seq (data not shown). This is in contrast to research on *C. albicans* that demonstrated that *SAP2* and *SAP5* mRNA was downregulated when exposed to similar concentrations of mucin in culture, despite their role in gut colonization[49]. The fact that *SAP2* and *SAP5* mRNA was downregulated in mucin culture and thus weakening the virulence of *C. albicans* could be explained by the inability of culture environments to permit adhesive, hyphal growth, which is tied to *SAP* expression[84]. Essentially, if environmental

conditions favour *C. albicans* filamentation and invasiveness as opposed to remaining persistent and commensal, the organism will become virulent and utilize virulence traits[50,139,140]. Therefore, the drastic upregulation of *YPS7* in yeast that has not adapted to a host gut environment provides evidence that *S. cerevisiae* may not follow the same regulatory constraints as its pathogenic counterpart.

The majority of research on Yps proteins investigate the growth impact of multiple *YPS* gene deletions under stress conditions[89,92]. My work was the first to look at *YPS* deletion mutants under a different carbon source than glucose. Creation of single, double and triple deletion mutants for the various *YPS* genes showed particular importance of the uncharacterized *YPS7* for growth on mucin medium (Figure 4B and 4C). Interestingly, deletion mutants for *YPS1* and *YPS3* which encode the Yps proteins with the highest amino acid sequence similarity to SAPs demonstrated very little or no growth defects on mucin medium (Figure 4B and 4C). This finding was in line with the qPCR data and suggests that *YPS7* induction is specific to the cellular response to growth on mucin.

Previous studies demonstrated Yps1 and Yps3 sub-cellular localization to be either at the plasma membrane or secreted into the extracellular environment[87,91], and their function is mainly attributed to the breakdown of misfolded GPI-anchored proteins under normal conditions[86]. In the presence of mucin, GFP-tagged Yps1, Yps3 and Yps7 was observed to be diffused throughout the cell (Figure 5A). There also appears to be an induction of Yps7-GFP in mucin conditions (Figure 5B). There may be a few reasons for this diffusion. Localization has yet to be tested for these proteins under carbon-limiting conditions. It may benefit the cell to direct proteolytic processes throughout the cytoplasm for resource scavenging in scarce conditions. This would be advantageous after the uptake of mucin glycoproteins from the environment. Yps7-GFP seems to be compartmentalized in the vacuole when cells are not grown in mucin (Figure 5A) and could

provide an example of mucin-specific proteolytic activity in the cytoplasm. In fact, high-content databases using fluorescence microscopy have demonstrated cytoplasmic localization for Yps1-GFP and Yps7-GFP, while Yps3-GFP seemed to be partially localized to the mitochondria even in normal growth conditions[122,129]. Yps3 may aid in the degradation of proteins at or within the mitochondria for proper import functioning, an important process for growth in stressed and non-stressed conditions as seen with the transcription factor Pdr3 (*see section 4.3*). Interestingly, truncated forms of Yps1 and Yps3, such that they do not possess the signalling peptide for transport to the plasma membrane, have been shown to still have proteolytic activity in the cytoplasm of cells[85,86]. As previously demonstrated with Yps3 by Olsen *et al.* (1999)[85], these truncations may just occur naturally and localize proteases to specific sites based on cellular needs. Preliminary western blots have demonstrated this may be the case, with small sized protein detected in Yps3-GFP WCE (Supplemental Figure S3). Further, it cannot be ruled out that protein transport may also be impacted in these carbon-limiting conditions, evident in the chemogenomic profile for *S. cerevisiae* growth in mucin (Figure 8). Nonetheless, it seems that Yps7 is the most important Yps protein for growth in mucin conditions.

The structure of dense mucin glycoproteins may induce osmotic stress on cells in growth media. Their abundance of carbohydrates surrounding the peptide core could cause a hyperosmotic response in cells. Cho *et al.* (2010)[92] demonstrated that combinatorial *YPS* deletion mutant strains (ie. deletion of three *YPS* genes or more) resulted in decreased tolerance to high salt concentrations in YPD. RNA-seq data also showed that *SKN7* was significantly downregulated by 9-fold in mucin conditions (Table 2). During hypo-osmotic stress, phosphorylation of the stress sensor Sln1 begins the phosphorelay cascade to Ypd1 and lastly to the transcription factor Skn7, a key regulator for the reinforcement of the cell wall[124]. Downregulation of *SKN7* suggests the activation of the opposing hyperosmotic stress (high osmolarity glycerol [HOG]) pathway in which

dephosphorylated Sln1 results in the blockage of the phosphorelay signal and accumulation of active dephosphorylated Ssk1, which induces expression of the mitogen-activated protein kinase Hog1[124]. However, there were no growth defects observed in *hog1*Δ when grown in mucin medium (Figure 6A). Moreover, though there seemed to be a partial rescue in *yps1*Δ*yps3*Δ*yps7*Δ cells grown in NaCl, overexpression of *HOG1* still did not rescue the growth defects observed in the majority of *yps7*Δ mutants in mucin medium (Figure 6A). Any potential osmotic stress induced by mucin does not appear to be the reason for *yps7*Δ mutant growth deficiency.

Other studies on *YPS* deletion mutants determined that conditions which impact the cell wall are detrimental to cell viability in these deletion mutants. Krysan *et al.* (2005)[89] looked at the impact on single *YPS* knockouts in the presence of cell wall disrupting compounds. Deletion of *YPS1* showed the most growth deficiency, affected by Congo Red disturbance of chitin/β-glucan fibril formation and caffeine induced cell wall stress, while deletion of *YPS7* showed unique growth deficiency to calcofluor white disruption of chitin polymer formation. My study was the first to investigate whether the gel-like polymeric structure of mucin in the growth medium could induce stress on the cell wall. There does seem to be cell wall stress induced by mucin at high temperatures, as seen in the *slt2*Δ control and mildly in *yps1*Δ*yps7*Δ (Figure 6B). The role *YPS1* plays in MAPK pathways[72] may be the reason for this slight growth deficiency and should be further explored in future studies. However, the growth deficiency observed in other *yps7*Δ mutants was not rescued upon the addition of 1 M sorbitol. Any mucin impact on cell wall integrity does not appear to be the main factor for growth deficiency in *yps7*Δ mutants.

Regulation for aspartyl proteases is not fully understood. In *C. albicans*, the regulation of SAPs is mainly correlated to virulent activity of the organism, such as during phenotypic switching to hyphal growth, or in the presence of extracellular host proteins[83]. For *S. cerevisiae*, Yps proteins are typically attributed to the response against cell wall stress[89], or the elevation of calcium/sodium

salts in the environment[141]. RNA-seq data suggests some evidence of the involvement of genes associated to pseudohyphal growth like *CDC65*, *STE20* and *DFG5* (Table 1 and 2). After testing for stresses that Yps proteins are known to be involved in, the growth deficiency observed in *yps7*Δ mutants may simply be their importance in the breakdown of mucin for uptake or eventual metabolism in the mitochondria. Directly linking Yps7 proteolytic activity to mucin breakdown will help understand how *S. cerevisiae* can metabolize mucin from the environment.

4.3 Impact of mucin on mitochondrial morphology and function

Exactly how mucin glycoproteins are broken down by yeast is still speculative. In such a stressful environment, cells are limited in carbohydrate sources that provide the cell with energy to grow and proliferate. By limiting carbon, genes in mitochondrial processes like the tricarboxylic acid cycle and oxidative phosphorylation are upregulated[60,61]. Mitochondria typically undergo fission and mitophagy during stress[103]. Moreover, yeast grown in carbon-limiting conditions in the presence of oxygen have been shown to demonstrate strictly respiratory glucose metabolism as well as have short and round mitochondria[106]. Similar conditions in the absence of oxygen have showed strictly fermentative glucose metabolism with large, branched mitochondria[106]. Through transcriptomics and chemogenomics screening, this work has demonstrated the importance of the mitochondria and cellular respiration for mucin metabolism.

The synthesis of ATP through oxidative phosphorylation concludes at the ATP synthase complex[142]. There was an enrichment of ATP synthase complex biogenesis (*ATP22*, *ATP23*, *OXA1*) in the list of top 50 upregulated genes (Figure 7A). Oxa1 acts as an insertase which embeds proteins from the mitochondrial matrix into the inner membrane[143]. Both Atp22 and Atp23 are inducers for the synthesis of Atp6, a subunit of the hydrophobic domain of the complex[144,145]. Atp6

is essential for ATP synthase activity and is hypothesized to produce the rotational force for the Oli1 ring of the hydrophobic domain, which transfers this coupling force to the hydrophilic catalytic domain for ATP synthesis[142]. This upregulation in proteins that support ATP synthase subunit insertion into the inner mitochondrial membrane, along with the upregulation of Atp6 inducers for increased complex activity, should also increase the amount of ATP synthesis within cells grown in mucin conditions.

Other effectors of mitochondrial structure and synthesis of electron transport chain units were also found in the RNA-seq data and chemogenomics screen. In fact, 11 of the top 50 upregulated genes are associated to mitochondrial function (Table 1). Among them, *MSS51* and *FIS1* were part of the enriched category for mitochondrial organization. Mss51 is important for Cox1 protein synthesis and incorporation into the cytochrome c oxidase complex[146]. Moreover, it was expected that in limited carbon conditions, mitochondrial fission would occur[106]. Fis1 is one of the main proteins involved in mitochondrial fission[147], and was found to be upregulated 4-fold in mucin conditions (Table 1). Indeed, live-cell fluorescence imaging using Cit1-RFP labelled strains showed induced short mitochondria in YPM compared to YPD (Figure 7A). Regarding the screen, this work revealed mitochondrial-associated genes that demonstrated better growth in YPM compared to their growth on YP, but still worse growth compared to the WT in YPM upon their deletion (*MZM1*, *QCR9*) (Figure 8). Among these, Mzm1 is a protein aiding in the assembly of cytochrome-bc1 complex[148]. Additionally, Qcr9 is one of the non-catalytic subunits of the cytochrome-bc1 complex that provides structural stability[149]. Since these deletion mutants demonstrated greater growth in YPM compared to YP, this may suggest that cells still benefit from having any carbon source in their growth medium. However, deletion mutants for these genes showed less growth in YPM compared to the WT strain (Supplemental Figure S5). This provides

further evidence that oxidative phosphorylation and the proper functioning of the electron transport chain is important for growth in mucin conditions.

Due to the presence of a carbon source, even as complex as mucin, it was expected that there would be mitochondrial-associated genes that when deleted, resulted in worse growth in the presence of mucin compared to no carbon source at all. From the chemogenomics screen, *CCM1* and *YCR095W-A* were genes that fit this profile and also grew worse in YPM compared to the WT upon their deletion (Figure 8 and Supplemental Figure S5). As mentioned previously, *CCM1* is involved in the stabilization of cytochrome-bc1 transcripts[128]. Its deletion is also known to result in a petite phenotype, meaning dysfunction in the metabolism of non-fermentable carbon sources[95]. *YCR095W-A* encodes for a protein of unknown function that has low localization signal to mitochondria[129]. WT mitochondria tagged with Cit1-RFP displayed short structures localized throughout the cell in mucin medium (Figure 9A), similar to yeast grown in ethanol or aerobic, glucose-limiting chemostat cultures[106]. As expected, deletion of *CCM1* and *YCR095W-A* resulted in similar mitochondrial morphology and further induction of mitochondrial biogenesis in YPM compared to YPD (Figure 9A and 9B). Regarding function, WT mitochondria increased OCR in the presence of mucin (Figure 10A), which can be attributed to the induction of mitochondrial biogenesis. Surprisingly, while deletion of *YCR095W-A* did not significantly impact OCR under water or ethanol conditions, there was a significant decrease in OCR in mucin conditions (Figure 10B). This result indicates that despite more mitochondria in the presence of mucin (Figure 9A and 9B), oxygen consumption was disrupted upon deletion of *YCR095W-A*. Unfortunately, no previous work has been conducted on this putative gene, and its amino acid sequence bears no resemblance to other proteins in *S. cerevisiae* S288C or other yeast species. The characterization of this protein, both in its structure and localization, could help determine a functional role during mucin metabolism and overall stress in carbon-limiting conditions.

Previous transcriptomics research has shown common regulation of *CCM1* and *YCR095W-A* by the transcription factor Pdr3[150,151]. Pdr3 is involved in the regulation of the pleiotropic drug response[152] and is a key component of the retrograde response in yeast, whereby mitochondrial signals influence nuclear gene expression[153]. *PDR3* is known to be induced transcriptionally during mitochondrial deficiency, and overexpression results in the suppression of mitochondrial import defects[154]. Pdr3 activation is also carbon source dependent, as it was demonstrated that BY4742 cells in a background lacking mitochondrial DNA inhibited *PDR3* transcription when grown in raffinose but not in glucose[155]. Moreover, it is attributed to the regulation of a large proportion of significantly differentially expressed genes (p = 1.09E-13)[156] under mucin conditions (data not shown). In fact, these large-scale studies showed that all known mitochondrial-associated genes that appeared in the top 50 lists and chemogenomics profile are regulated in some way by Pdr3[150,151]. Therefore, furthering work on Pdr3 may elucidate an active role in the regulation of genes as a response to signals from mitochondria during growth in mucin conditions.

5.0 Conclusion

In this study, I sought to determine whether *S. cerevisiae* can utilize mucin as an energy source and the key processes that permit the yeast to grow, similar to other fungi that colonize the human gut. Through classical growth assays, RNA sequencing and chemogenomics screening methods, this work showed that even the common laboratory *S. cerevisiae* S288C strain can grow in media with mucin as the main carbon source. This work also identified the importance of the aspartyl protease Yps7 to grow in mucin media and further characterized the morphological and transcriptomic impact on cells grown in mucin conditions. These remodelling events shed light on the significance of the mitochondria for cells to grow and metabolize mucin, and determined the specific importance of the putative protein Ycr095w-a for growth on mucin. This work complements previous microbiome research which mainly uses culture-independent metagenomics techniques and supports *S. cerevisiae* as a gut colonizer as opposed to just an environmental organism passing through the GI tract. By understanding how the most common dietary fungus can live in a mucin-rich environment, we can further our knowledge on the interactions occurring in the gut microbiome that impact human health.

6.0 References

1. Shreiner, A. B., Kao, J. Y. & Young, V. B. The gut microbiome in health and in disease. *Curr. Opin. Gastroenterol.* **31**, 69–75 (2015).
2. Cani, P. D. Human gut microbiome: Hopes, threats and promises. *Gut* **67**, 1716–1725 (2018).
3. Peterson, J. *et al.* The NIH Human Microbiome Project. *Genome Res.* **19**, 2317–2323 (2009).
4. Methé, B. A. *et al.* A framework for human microbiome research. *Nature* **486**, 215–221 (2012).
5. Turnbaugh, P. J. *et al.* The Human Microbiome Project. *Nature* **449**, 804–810 (2007).
6. Qin, J. *et al.* A human gut microbial gene catalogue established by metagenomic sequencing. *Nature* **464**, 59–65 (2010).
7. Turnbaugh, P. J. *et al.* A core gut microbiome in obese and lean twins. *Nature* **457**, 480–484 (2009).
8. Kurokawa, K. *et al.* Comparative metagenomics revealed commonly enriched gene sets in human gut microbiomes. *DNA Res.* **14**, 169–181 (2007).
9. Petersen, C. & Round, J. L. Defining dysbiosis and its influence on host immunity and disease. *Cell. Microbiol.* **16**, 1024–1033 (2014).
10. Lloyd-Price, J., Abu-Ali, G. & Huttenhower, C. The healthy human microbiome. *Genome Med.* **8**, 1–11 (2016).
11. Moya, A. & Ferrer, M. Functional Redundancy-Induced Stability of Gut Microbiota Subjected to Disturbance. *Trends Microbiol.* **24**, 402–413 (2016).
12. Ott, S. J. *et al.* Fungi and inflammatory bowel diseases: Alterations of composition and diversity. *Scand. J. Gastroenterol.* **43**, 831–841 (2008).
13. Iliev, I. D. *et al.* Interactions between commensal fungi and the C-type lectin receptor dectin-1 influence colitis. *Science (80-.).* **336**, 1314–1317 (2012).
14. Hoffmann, C. *et al.* Archaea and Fungi of the Human Gut Microbiome: Correlations with Diet and Bacterial Residents. *PLoS One* **8**, (2013).
15. Hallen-Adams, H. E., Kachman, S. D., Kim, J., Legge, R. M. & Martínez, I. Fungi inhabiting the healthy human gastrointestinal tract: A diverse and dynamic community. *Fungal Ecol.* **15**, 9–17 (2015).
16. Sokol, H. *et al.* Fungal microbiota dysbiosis in IBD. *Gut* **66**, 1039–1048 (2017).
17. David, L. A. *et al.* Diet rapidly and reproducibly alters the human gut microbiome. *Nature* **505**, 559–563 (2014).
18. Hillman, E. T., Lu, H., Yao, T. & Nakatsu, C. H. Microbial ecology along the gastrointestinal tract. *Microbes Environ.* **32**, 300–313 (2017).
19. Nash, A. K. *et al.* The gut mycobiome of the Human Microbiome Project healthy cohort. *Microbiome* **5**, 153 (2017).
20. Strati, F. *et al.* Age and gender affect the composition of fungal population of the human gastrointestinal tract. *Front. Microbiol.* **7**, 1–16 (2016).
21. Hatoum, R., Labrie, S. & Fliss, I. Antimicrobial and probiotic properties of yeasts: From fundamental to novel applications. *Front. Microbiol.* **3**, 1–12 (2012).
22. Hallen-Adams, H. E. & Suhr, M. J. Fungi in the healthy human gastrointestinal tract. *Virulence* **8**, 352–358 (2017).
23. Huffnagle, G. B. & Noverr, M. C. The emerging world of the fungal microbiome. *Trends Microbiol.* **21**, 334–341 (2013).
24. Hall, R. A. & Noverr, M. C. Fungal interactions with the human host: exploring the spectrum

of symbiosis. *Curr. Opin. Microbiol.* **40**, 58–64 (2017).
25. Struyf, N. *et al.* Bread Dough and Baker's Yeast: An Uplifting Synergy. *Compr. Rev. Food Sci. Food Saf.* **16**, 850–867 (2017).
26. Walker, G. & Stewart, G. Saccharomyces cerevisiae in the Production of Fermented Beverages. *Beverages* **2**, 30 (2016).
27. Edwards-Ingram, L. *et al.* Genotypic and physiological characterization of Saccharomyces boulardii, the probiotic strain of Saccharomyces cerevisiae. *Appl. Environ. Microbiol.* **73**, 2458–2467 (2007).
28. Sivignon, A. *et al.* Saccharomyces cerevisiaeCNCMI-3856 prevents colitis induced by AIEC bacteria in the transgenic mouse model mimicking Crohn's disease. *Inflamm. Bowel Dis.* **21**, 276–286 (2015).
29. Chiaro, T. R. *et al.* A member of the gut mycobiota modulates host purine metabolism exacerbating colitis in mice. *Sci. Transl. Med.* **9**, eaaf9044 (2017).
30. Chehoud, C. *et al.* Fungal signature in the gut microbiota of pediatric patients with inflammatory bowel disease. *Inflamm. Bowel Dis.* **21**, 1948–1956 (2015).
31. Li, Q. *et al.* Dysbiosis of gut fungal microbiota is associated with mucosal inflammation in crohn's disease. *J. Clin. Gastroenterol.* **48**, 513–523 (2014).
32. Liguori, G. *et al.* Fungal dysbiosis in mucosa-associated microbiota of Crohn's disease patients. *J. Crohn's Colitis* **10**, 296–305 (2016).
33. Willis, K. A. *et al.* Fungi form interkingdom microbial communities in the primordial human gut that develop with gestational age. *FASEB journal : official publication of the Federation of American Societies for Experimental Biology* **33**, 12825–12837 (2019).
34. Borges, F. M. *et al.* Fungal Diversity of Human Gut Microbiota Among Eutrophic, Overweight, and Obese Individuals Based on Aerobic Culture-Dependent Approach. *Curr. Microbiol.* **75**, 726–735 (2018).
35. Kim, S. H. *et al.* Global Analysis of the Fungal Microbiome in Cystic Fibrosis Patients Reveals Loss of Function of the Transcriptional Repressor Nrg1 as a Mechanism of Pathogen Adaptation. *PLoS Pathog.* **11**, 1–26 (2015).
36. He, G. *et al.* Noninvasive measurement of anatomic structure and intraluminal oxygenation in the gastrointestinal tract of living mice with spatial and spectral EPR imaging. *Proc. Natl. Acad. Sci. U. S. A.* **96**, 4586–4591 (1999).
37. FALLINGBORG, J. *et al.* pH-Profile and regional transit times of the normal gut measured by a radiotelemetry device. *Aliment. Pharmacol. Ther.* **3**, 605–614 (2007).
38. Johansson, M. E. V., Sjövall, H. & Hansson, G. C. The gastrointestinal mucus system in health and disease. *Nat. Rev. Gastroenterol. Hepatol.* **10**, 352–361 (2013).
39. Bansil, R. Mucin Biophysics. *Annu. Rev. Physiol.* **57**, 635–657 (1995).
40. Johansson, M. E. V & Hansson, G. C. Preservation of Mucus in Histological Sections. **842**, 229–235 (2012).
41. Rhodes, J. M. Colonic mucus and mucosal glycoproteins: the key to colitis and cancer? *Gut* **30**, 1660–1666 (1989).
42. Hattrup, C. L. & Gendler, S. J. Structure and Function of the Cell Surface (Tethered) Mucins. *Annu. Rev. Physiol.* **70**, 431–457 (2008).
43. Thornton, D. J., Rousseau, K. & McGuckin, M. A. Structure and Function of the Polymeric Mucins in Airways Mucus. *Annu. Rev. Physiol.* **70**, 459–486 (2008).
44. Johansson, M. E. V. *et al.* Composition and functional role of the mucus layers in the intestine. *Cell. Mol. Life Sci.* **68**, 3635–3641 (2011).
45. Hansson, G. C. & Johansson, M. E. V. The inner of the two Muc2 mucin-dependent mucus

layers in colon is devoid of bacteria. *Gut Microbes* **1**, 51–54 (2010).
46. Yeung, A. T. Y., Parayno, A. & Hancock, R. E. W. Mucin Promotes Rapid Surface Motility in. **3**, 1–12 (2012).
47. Bendiak, G. N. & Ratjen, F. The approach to pseudomonas aeruginosa in cystic fibrosis. *Semin. Respir. Crit. Care Med.* **30**, 587–595 (2009).
48. Flynn, J. M., Niccum, D., Dunitz, J. M. & Hunter, R. C. Evidence and Role for Bacterial Mucin Degradation in Cystic Fibrosis Airway Disease. *PLoS Pathog.* **12**, 1–21 (2016).
49. Kavanaugh, N. L., Zhang, A. Q., Nobile, C. J., Johnson, A. D. & Ribbeck, K. Mucins suppress virulence traits of Candida albicans. *MBio* **5**, 1–8 (2014).
50. Böhm, L. *et al.* The yeast form of the fungus Candida albicans promotes persistence in the gut of gnotobiotic mice. *PLoS Pathog.* **13**, 1–26 (2017).
51. Jacobsen, I. D. *et al.* Candida albicans dimorphism as a therapeutic target. *Expert Rev. Anti. Infect. Ther.* **10**, 85–93 (2012).
52. Moyes, D. L. *et al.* A biphasic innate immune MAPK response discriminates between the yeast and hyphal forms of candida albicans in epithelial cells. *Cell Host Microbe* **8**, 225–235 (2010).
53. Sudbery, P. E. Growth of Candida albicans hyphae. *Nat. Rev. Microbiol.* **9**, 737–748 (2011).
54. Taymaz-Nikerel, H., Cankorur-Cetinkaya, A. & Kirdar, B. Genome-wide transcriptional response of Saccharomyces cerevisiae to stress-induced perturbations. *Front. Bioeng. Biotechnol.* **4**, (2016).
55. DeRisi, J. L., Iyer, V. R. & Brown, P. O. Exploring the metabolic and genetic control of gene expression on a genomic scale. *Chemtracts* **12**, 148–152 (1999).
56. Boorstein, S. A. & Godierman, M. Theory for zero-field splittings in aromatic hydrocarbons. III. *J. Chem. Phys.* **39**, 2443–2452 (1963).
57. Zaman, S., Lippman, S. I., Schneper, L., Slonim, N. & Broach, J. R. Glucose regulates transcription in yeast through a network of signaling pathways. *Mol. Syst. Biol.* **5**, 1–14 (2009).
58. Livas, D., Almering, M. J. H., Daran, J. M., Pronk, J. T. & Gancedo, J. M. Transcriptional responses to glucose in Saccharomyces cerevisiae strains lacking a functional protein kinase A. *BMC Genomics* **12**, 1–12 (2011).
59. Teixeira, M. C., Mira, N. P. & Sá-Correia, I. A genome-wide perspective on the response and tolerance to food-relevant stresses in Saccharomyces cerevisiae. *Curr. Opin. Biotechnol.* **22**, 150–156 (2011).
60. Boer, V. M., De Winde, J. H., Pronk, J. T. & Piper, M. D. W. The genome-wide transcriptional responses of Saccharomyces cerevisiae grown on glucose in aerobic chemostat cultures limited for carbon, nitrogen, phosphorus, or sulfur. *J. Biol. Chem.* **278**, 3265–3274 (2003).
61. Wu, J., Zhang, N., Hayes, A., Panoutsopoulo, K. & Oliver, S. G. Global analysis of nutrient control of gene expression in Saccharomyces cerevisiae during growth and starvation. *Proc. Natl. Acad. Sci. U. S. A.* **101**, 3148–3153 (2004).
62. Conrad, M. *et al.* Nutrient sensing and signaling in the yeast Saccharomyces cerevisiae. *FEMS Microbiol. Rev.* **38**, 254–299 (2014).
63. Özcan, S., Dover, J., Rosenwald, A. G., Wölfl, S. & Johnston, M. Two glucose transporters in Saccharomyces cerevisiae are glucose sensors that generate a signal for induction of gene expression. *Proc. Natl. Acad. Sci. U. S. A.* **93**, 12428–12432 (1996).
64. Ljungdahl, P. O. Amino-acid-induced signalling via the SPS-sensing pathway in yeast. *Biochem. Soc. Trans.* **37**, 242–247 (2009).

65. Bastidas, R. J. & Heitman, J. Fungal Virulence. *Proc. Natl. Acad. Sci. United States Am.* **106**, 351–352 (2009).
66. Cullen, J., Irick, M. M., Neal, C., Delrow, J. & George, F. Msb2 is a Signaling Mucin at the Head of the Filamentous Growth Pathway. *Genes Dev.* **18**, 1695–1708 (2004).
67. Gimeno, C. J., Ljungdahl, P. O., Styles, C. A. & Fink, G. R. Unipolar cell divisions in the yeast S. cerevisiae lead to filamentous growth: Regulation by starvation and RAS. *Cell* **68**, 1077–1090 (1992).
68. Mösch, H. U., Roberts, R. L. & Fink, G. R. Ras2 signals via the Cdc42/Ste20/mitogen-activated protein kinase module to induce filamentous growth in Saccharomyces cerevisiae. *Proc. Natl. Acad. Sci. U. S. A.* **93**, 5352–5356 (1996).
69. Lo, W. & Dranginis, A. M. Flo11.pdf. *Mol. Biol. Cell* **9**, 161–171 (1998).
70. Ryan, O. *et al.* Global gene deletion analysis exploring yeast filamentous growth. *Science (80-.).* **337**, 1352–1356 (2012).
71. Karunanithi, S. & Cullen, P. J. The filamentous growth MAPK pathway responds to glucose starvation through the Mig1/2 transcriptional repressors in saccharomyces cerevisiae. *Genetics* **192**, 869–887 (2012).
72. Vadaie, N. *et al.* Cleavage of the signaling mucin Msb2 by the aspartyl protease Yps1 is required for MAPK activation in yeast. *J. Cell Biol.* **181**, 1073–1081 (2008).
73. Galcheva-Gargova, Z., Dérijard, B., Wu, I. H. & Davis, R. J. An osmosensing signal transduction pathway in mammalian cells. *Science (80-.).* **265**, 806–808 (1994).
74. Elferink, J. G. R. The effect of ethylenediaminetetraacetic acid on yeast cell membranes. *Protoplasma* **80**, 261–268 (1974).
75. Costanzo, M. *et al.* A global genetic interaction network maps a wiring diagram of cellular function. *Science (80-.).* **353**, (2016).
76. Höfs, S., Mogavero, S. & Hube, B. Interaction of Candida albicans with host cells: virulence factors, host defense, escape strategies, and the microbiota. *J. Microbiol.* **54**, 149–169 (2016).
77. Davies, D. R. The structure and function of the aspartic proteinases. *Annu. Rev. Biophys. Biophys. Chem.* **19**, 189–215 (1990).
78. De Repentigny, L., Aumont, F., Bernard, K. & Belhumeur, P. Characterization of binding of Candida albicans to small intestinal mucin and its role in adherence to mucosal epithelial cells. *Infect. Immun.* **68**, 3172–3179 (2000).
79. Meiller, T. F. *et al.* A novel immune evasion strategy of Candida albicans: Proteolytic cleavage of a salivary antimicrobial peptide. *PLoS One* **4**, (2009).
80. Bochenska, O. *et al.* The action of ten secreted aspartic proteases of pathogenic yeast Candida albicans on major human salivary antimicrobial peptide, histatin 5. *Acta Biochim. Pol.* **63**, 403–410 (2016).
81. Frank, C. F. & Hostetter, M. K. Cleavage of E-cadherin: a mechanism for disruption of the intestinal epithelial barrier by Candida albicans. *Transl. Res.* **149**, 211–222 (2007).
82. Colina, A.-R., Aumont, F., Deslauriers, N., Belhumeur, P. & De Repentigny, L. Evidence for Degradation of Gastrointestinal Mucin by Candida albicans Secretory Aspartyl Proteinase. *Infect. Immun.* **64**, 4514–4519 (1996).
83. Hube, B., Monod, M., Schofield, D. A., Brown, A. J. P. & Gow, N. A. R. Expression of seven members of the gene family encoding secretory aspartyl proteinases in Candida albicans. *Mol. Microbiol.* **14**, 87–99 (1994).
84. Pappas, P. G. *et al.* Treatment of oropharyngeal and esophageal candidiasis. *Uptodate* **67**, 1–12 (2016).

85. Olsen, V., Cawley, N. X., Brandt, J., Egel-Mitani, M. & Loh, Y. P. Identification and characterization of Saccharomyces cerevisiae yapsin 3, a new member of the yapsin family of aspartic proteases encoded by the YPS3 gene. *Biochem. J.* **339**, 407–411 (1999).
86. Gagnon-Arsenault, I., Parisé, L., Tremblay, J. & Bourbonnais, Y. Activation mechanism, functional role and shedding of glycosylphosphatidylinositol-anchored Yps1p at the Saccharomyces cerevisiae cell surface. *Mol. Microbiol.* **69**, 982–993 (2008).
87. Smeekens, J. M., Xiao, H. & Wu, R. Global Analysis of Secreted Proteins and Glycoproteins in Saccharomyces cerevisiae. *Journal of Proteome Research* **16**, 1039–1049 (2017).
88. Gagnon-Arsenault, I., Tremblay, J. & Bourbonnais, Y. Fungal yapsins and cell wall: A unique family of aspartic peptidases for a distinctive cellular function. *FEMS Yeast Res.* **6**, 966–978 (2006).
89. Krysan, D. J., Ting, E. L., Abeijon, C., Kroos, L. & Fuller, R. S. Yapsins are a family of aspartyl proteases required for cell wall integrity in Saccharomyces cerevisiae. *Eukaryot. Cell* **4**, 1364–1374 (2005).
90. Heinisch, J. J., Lorberg, A., Schmitz, H. P. & Jacoby, J. J. The protein kinase C-mediated MAP kinase pathway involved in the maintenance of cellular integrity in Saccharomyces cerevisiae. *Mol. Microbiol.* **32**, 671–680 (1999).
91. Dubé, A. K., Bélanger, M., Gagnon-Arsenault, I. & Bourbonnais, Y. N-terminal entrance loop of yeast Yps1 and O-glycosylation of substrates are determinant factors controlling the shedding activity of this GPI-anchored endopeptidase Microbial biochemistry, physiology and metabolism. *BMC Microbiol.* **15**, 1–14 (2015).
92. Cho, E. Y. *et al.* Multiple-yapsin-deficient mutant strains for high-level production of intact recombinant proteins in Saccharomyces cerevisiae. *J. Biotechnol.* **149**, 1–7 (2010).
93. Saraste, M. Oxidative phosphorylation at the fin de siecle. *Science (80-.).* **283**, 1488–1493 (1999).
94. Dimmer, K. S. *et al.* Genetic Basis of Mitochondrial Function and Morphology in Saccharomyces cerevisiae. *Mol. Biol. Cell* **13**, 847–853 (2002).
95. Merz, S. & Westermann, B. Genome-wide deletion mutant analysis reveals genes required for respiratory growth, mitochondrial genome maintenance and mitochondrial protein synthesis in Saccharomyces cerevisiae. *Genome Biol.* **10**, (2009).
96. Bolotin-Fukuhara, M. & Grivell, L. A. Genetic approaches to the study of mitochondrial biogenesis in yeast. *Antonie Van Leeuwenhoek* **62**, 131–153 (1992).
97. Przybyla-Zawislak, B., Gadde, D. M., Ducharme, K. & McCammon, M. T. Genetic and biochemical interactions involving tricarboxylic acid cycle (TCA) function using a collection of mutants defective in all TCA cycle genes. *Genetics* **152**, 153–166 (1999).
98. Pfanner, N. & Geissler, A. Versatility of the mitochondrial protein import machinery. *Nat. Rev. Mol. Cell Biol.* **2**, 339–349 (2001).
99. Fox, T. D. An MBoC favorite: mitochondrial transmission during mating in Saccharomyces cerevisiae is determined by mitochondrial fusion and fission and the intramitochondrial segregation of mitochondrial DNA. *Mol. Biol. Cell* **23**, 4144 (2012).
100. Okamoto, K. & Shaw, J. M. Mitochondrial Morphology and Dynamics in Yeast and Multicellular Eukaryotes. *Annual Review of Genetics* **39**, 503–536 (2005).
101. Shaw, J. M. & Nunnari, J. Mitochondrial dynamics and division in budding yeast. *Trends Cell Biol.* **12**, 178–184 (2002).
102. Hackenbrock, C. R. Ultrastructural bases for metabolically linked mechanical activity in mitochondria. I. Reversible ultrastructural changes with change in metabolic steady state in isolated liver mitochondria. *J. Cell Biol.* **30**, 269–297 (1966).

103. May, A. I., Devenish, R. J. & Prescott, M. The many faces of mitochondrial autophagy: Making sense of contrasting observations in recent research. *Int. J. Cell Biol.* **2012**, (2012).
104. Kanki, T. & Klionsky, D. J. Mitophagy in yeast occurs through a selective mechanism. *J. Biol. Chem.* **283**, 32386–32393 (2008).
105. Mao, K., Wang, K., Zhao, M., Xu, T. & Klionsky, D. J. Two MAPK-signaling pathways are required for mitophagy in Saccharomyces cerevisiae. *J. Cell Biol.* **193**, 755–767 (2011).
106. Visser, W. *et al.* Effects of growth conditions on mitochondrial morphology in Saccharomyces cerevisiae. *Antonie Van Leeuwenhoek* **67**, 243–253 (1995).
107. Longtine, M. S. *et al.* Additional Modules for Versatile and Economical PCR-based Gene Deletion and Modification in Saccharomyces cerevisiae. *Yeast* **14**, 953–961 (2018).
108. Winzeler, E. A. *et al.* Analysis Linked references are available on JSTOR for this article : Functional Characterization of the S . cerevisiae Genome by Gene Deletion and Parallel Analysis. *Science (80-.).* **285**, 901–906 (1999).
109. Ghaemmaghami, S. *et al.* Global analysis of protein expression in yeast. *Nature* **425**, 737–741 (2003).
110. Glenister, D. A., Salamon, K. E., Smith, K., Beighton, D. & Keevil, C. W. Enhanced growth of complex communities of dental plaque bacteria in mucin-limited continuous culture. *Microbial Ecology in Health and Disease* **1**, 31–38 (1988).
111. Terra, V. S., Homer, K. A., Rao, S. G., Andrew, P. W. & Yesilkaya, H. Characterization of novel β-galactosidase activity that contributes to glycoprotein degradation and virulence in Streptococcus pneumoniae. *Infect. Immun.* **78**, 348–357 (2010).
112. Livak, K. J. & Schmittgen, T. D. Analysis of relative gene expression data using real-time quantitative PCR and the 2-ΔΔCT method. *Methods* **25**, 402–408 (2001).
113. Kao, C. F. & Osley, M. A. In vivo assays to study histone ubiquitylation. *Methods* **31**, 59–66 (2003).
114. McCloy, R. A. *et al.* Partial inhibition of Cdk1 in G2 phase overrides the SAC and decouples mitotic events. *Cell Cycle* **13**, 1400–1412 (2014).
115. Dobin, A. *et al.* STAR: Ultrafast universal RNA-seq aligner. *Bioinformatics* **29**, 15–21 (2013).
116. Love, M. I., Huber, W. & Anders, S. Moderated estimation of fold change and dispersion for RNA-seq data with DESeq2. *Genome Biol.* **15**, 1–21 (2014).
117. Bolger, A. M., Lohse, M. & Usadel, B. Trimmomatic: A flexible trimmer for Illumina sequence data. *Bioinformatics* **30**, 2114–2120 (2014).
118. Roberts, A., Pimentel, H., Trapnell, C. & Pachter, L. Identification of novel transcripts in annotated genomes using RNA-seq. *Bioinformatics* **27**, 2325–2329 (2011).
119. Huang, D. W., Sherman, B. T. & Lempicki, R. A. Systematic and integrative analysis of large gene lists using DAVID bioinformatics resources. *Nat. Protoc.* **4**, 44–57 (2009).
120. Liu, W., Wang, B., Chen, L., Chen, K. & Wang, J. Research of demand recognition based on template matching. *ICCSE 2016 - 11th Int. Conf. Comput. Sci. Educ.* **41**, 573–577 (2016).
121. Srikumar, T. *et al.* Global analysis of SUMO chain function reveals multiple roles in chromatin regulation. *J. Cell Biol.* **201**, 145–163 (2013).
122. Koh, J. L. Y. *et al.* CYCLoPs: A comprehensive database constructed from automated analysis of protein abundance and subcellular localization patterns in Saccharomyces cerevisiae. *G3 Genes, Genomes, Genet.* **5**, 1223–1232 (2015).
123. Kraus, O. Z. *et al.* Automated analysis of high-content microscopy data with deep learning. *Mol. Syst. Biol.* **13**, 924 (2017).
124. Levin, D. E. Cell Wall Integrity Signaling in Saccharomyces cerevisiae Cell Wall as a Target

for Antifungal Drug Development. *Microbiol. Mol. Biol. Rev.* **69**, 262–291 (2005).
125. Tong, A. H. Y. *et al.* Global Mapping of the Yeast Genetic Interaction Network. *Science (80-.).* **303**, 808–813 (2004).
126. Górka-Nieć, W., Perlińska-Lenart, U., Zembek, P., Palamarczyk, G. & Kruszewska, J. S. Influence of sorbitol on protein production and glycosylation and cell wall formation in Trichoderma reesei. *Fungal Biol.* **114**, 855–862 (2010).
127. Martín, H. *et al.* Molecular and functional characterization of a mutant allele of the mitogen-activated protein-kinase gene SLT2(MPK1) rescued from yeast autolytic mutants. *Curr. Genet.* **29**, 516–522 (1996).
128. Moreno, J. I., Buie, K. S., Price, R. E. & Piva, M. A. Ccm1p/Ygr150cp, a pentatricopeptide repeat protein, is essential to remove the fourth intron of both COB and COX1 pre-mRNAs in Saccharomyces cerevisiae. *Curr. Genet.* **55**, 475–484 (2009).
129. Breker, M., Gymrek, M., Moldavski, O. & Schuldiner, M. LoQAtE - Localization and Quantitation ATlas of the yeast proteomE. A new tool for multiparametric dissection of single-protein behavior in response to biological perturbations in yeast. *Nucleic Acids Res.* **42**, 1–5 (2014).
130. Kim, K. S., Rosenkrantz, M. S. & Guarente, L. Saccharomyces cerevisiae contains two functional citrate synthase genes. *Mol. Cell. Biol.* **6**, 1936–1942 (1986).
131. Higuchi-Sanabria, R. *et al.* Characterization of fluorescent proteins for three- and four-color live-cell imaging in S. cerevisiae. *PLoS One* **11**, 1–15 (2016).
132. Tsubaki, M. & Yoshikawa, S. Fourier-Transform Infrared Study of Azide Binding to the Fea3-CuB Binuclear Site of Bovine Heart Cytochrome c Oxidase: New Evidence for a Redox-Linked Conformational Change at the Binuclear Site. *Biochemistry* **32**, 174–182 (1993).
133. Johnston, G. C., Ehrhardt, C. W., Lorincz, A. & Carter, B. L. A. Regulation of cell size in the yeast Saccharomyces cerevisiae. *J. Bacteriol.* **137**, 1–5 (1979).
134. Edenberg, E. R., Mark, K. G. & Toczyski, D. P. Ndd1 Turnover by SCFGrr1 Is Inhibited by the DNA Damage Checkpoint in Saccharomyces cerevisiae. *PLoS Genet.* **11**, 1–16 (2015).
135. McMurray, M. A. *et al.* Septin Filament Formation Is Essential in Budding Yeast. *Dev. Cell* **20**, 540–549 (2011).
136. Peggie, M. W. *et al.* Essential functions of Sds22p in chromosome stability and nuclear localization of PP1. *J. Cell Sci.* **115**, 195–206 (2002).
137. Marion, R. M. *et al.* Sfp1 is a stress- and nutrient-sensitive regulator of ribosomal protein gene expression. *Proc. Natl. Acad. Sci. U. S. A.* **101**, 14315–14322 (2004).
138. Fabrizio, P., Pozza, F., Pletcher, S. D., Gendron, C. M. & Longo, V. D. Regulation of longevity and stress resistance by Sch9 in yeast. *Science (80-.).* **292**, 288–290 (2001).
139. Rapala-Kozik, M. *et al.* Extracellular proteinases of Candida species pathogenic yeasts. *Mol. Oral Microbiol.* **33**, 113–124 (2018).
140. De Bernardis, F. *et al.* High aspartyl proteinase production and vaginitis in human immunodeficiency virus-infected women. *J. Clin. Microbiol.* **37**, 1376–1380 (1999).
141. Mazur, P. *et al.* Differential expression and function of two homologous subunits of yeast 1,3-beta-D-glucan synthase. *Mol. Cell. Biol.* **15**, 5671–5681 (1995).
142. Ko, Y. H., Hullihen, J., Hong, S. & Pedersen, P. L. Mitochondrial F0F1 ATP synthase. Subunit regions on the F1 motor shielded by F0, functional significance, and evidence for an involvement of the unique F0 subunit F6. *J. Biol. Chem.* **275**, 32931–32939 (2000).
143. Herrmann, J. M., Neupert, W. & Stuart, R. A. Insertion into the mitochondrial inner membrane of a polytopic protein, the nuclear-encoded Oxa1p. *EMBO J.* **16**, 2217–2226

(1997).
144. Zeng, X., Hourset, A. & Tzagoloff, A. The Saccharomyces cerevisiae ATP22 gene codes for the mitochondrial ATPase subunit 6-specific translation factor. *Genetics* **175**, 55–63 (2007).
145. Lim, J. *et al.* An Essential Role for Talin during ⌴ M ␑ 2 -mediated Phagocytosis. *Mol. Biol. Cell* **18**, 976–985 (2007).
146. Perez-Martinez, X., Broadley, S. A. & Fox, T. D. Mss51p promotes mitochondrial Cox1p synthesis and interacts with newly synthesized Cox1p. *EMBO J.* **22**, 5951–5961 (2003).
147. Mozdy, A. D., McCaffery, J. M. & Shaw, J. M. Dnm1p GTPase-mediated mitochondrial fission is a multi-step process requiring the novel integral membrane component Fis1p. *J. Cell Biol.* **151**, 367–379 (2000).
148. Atkinson, A. *et al.* Mzm1 influences a labile pool of mitochondrial zinc important for respiratory function. *J. Biol. Chem.* **285**, 19450–19459 (2010).
149. Phillips, J. D., Schmitt, M. E., Brown, T. A., Beckmann, J. D. & Trumpower, B. L. Isolation and characterization of QCR9, a nuclear gene encoding the 7.3-kDa subunit 9 of the Saccharomyces cerevisiae ubiquinol-cytochrome c oxidoreductase complex. An intron-containing gene with a conserved sequence occurring in the intron of COX4. *J. Biol. Chem.* **265**, 20813–20821 (1990).
150. Salin, H. *et al.* Structure and properties of transcriptional networks driving selenite stress response in yeasts. *BMC Genomics* **9**, 1–14 (2008).
151. Weidberg, H. & Amon, A. MitoCPR—A surveillance pathway that protects mitochondria in response to protein import stress. *Science (80-.).* **360**, (2018).
152. Delaveau, T., Delahodde, A., Carvajal, E., Subik, J. & Jacq, C. PDR3, a new yeast regulatory gene, is homologous to PDR1 and controls the multidrug resistance phenomenon. *MGG Mol. Gen. Genet.* **244**, 501–511 (1994).
153. Epstein, C. B. *et al.* Genome-wide responses to mitochondrial dysfunction. *Mol. Biol. Cell* **12**, 297–308 (2001).
154. Koh, J. Y., Hajek, P. & Bedwell, D. M. Overproduction of PDR3 Suppresses Mitochondrial Import Defects Associated with a TOM70 Null Mutation by Increasing the Expression of TOM72 in Saccharomyces cerevisiae. *Mol. Cell. Biol.* **21**, 7576–7586 (2001).
155. Devaux, F., Carvajal, E., Moye-Rowley, S. & Jacq, C. Genome-wide studies on the nuclear PDR3-controlled response to mitochondrial dysfunction in yeast. *FEBS Lett.* **515**, 25–28 (2002).
156. Teixeira, M. C. *et al.* YEASTRACT: An upgraded database for the analysis of transcription regulatory networks in Saccharomyces cerevisiae. *Nucleic Acids Res.* **46**, D348–D353 (2018).
157. Brachmann, C. B. *et al.* Designer deletion strains derived from Saccharomyces cerevisiae S288C: A useful set of strains and plasmids for PCR-mediated gene disruption and other applications. *Yeast* **14**, 115–132 (1998).
158. Christianson, T. W., Sikorski, R. S., Dante, M., Shero, J. H. & Hieter, P. Multifunctional yeast high-copy-number shuttle vectors. *Gene* **110**, 119–122 (1992).
159. Ho, C. H. *et al.* A molecular barcoded yeast ORF library enables mode-of-action analysis of bioactive compounds. *Nat. Biotechnol.* **27**, 369–377 (2009).
160. Dacquay, L. *et al.* NuA4 lysine acetyltransferase complex contributes to phospholipid homeostasis in Saccharomyces cerevisiae. *G3 Genes, Genomes, Genet.* **7**, 1799–1809 (2017).

161. Teste, M. A., Duquenne, M., François, J. M. & Parrou, J. L. Validation of reference genes for quantitative expression analysis by real-time RT-PCR in Saccharomyces cerevisiae. *BMC Mol. Biol.* **10**, 99 (2009).

7.0 Contributions of Collaborators

Genome Quebec performed the RNA-sequencing experiments and the Canadian Centre for Computational Genomics (C3G) curated the differential expression data using sequencing reads. Dylan Singh, an undergraduate student in the Translational Molecular Medicine program, conducted the qRT-PCR experiments.

8.0 Appendices

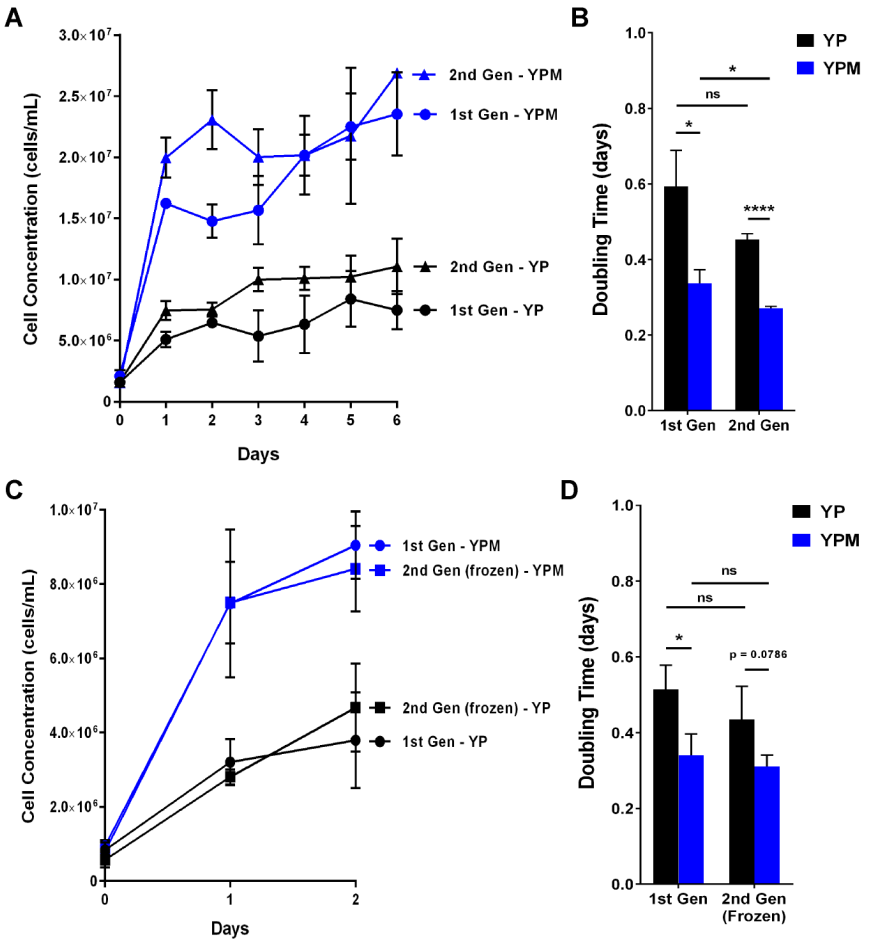

Supplemental Figure S1 *S. cerevisiae* can grow and temporarily adapt to mucin media. (A) WT (YKB1117) cells were grown to mid log phase in YPD, washed in YP and reinoculated into 50 mL of YP (black) and YPM (blue) media (1st Gen, ●). Cultures were incubated for six days at 30°C and cell concentration was measured via cell counting on a hemocytometer by aliquoting 100 uL of culture every 24 hrs. After six days, YPM cells were harvested, washed in YP and reinoculated into 50 mL of new YP and YPM media (2nd Gen, ▲). Growth of cell cultures were measured similarly. (B) 2nd Gen cells improved doubling time in mucin media, quantified during exponential growth phase from 0-1 days. (C) Frozen 2nd Gen cells (■) lost their adaptive growth ability. 2nd Gen YPM cells were stored after six days of growth in YPD + 15% glycerol at -80°C. These cells were revived on YPD agar plates, grown to mid log phase in YPD, washed in YP and reinoculated into 10 mL of YP and YPM media. Cultures were incubated for two days at 30°C and growth of cell cultures were measured similarly. (D) 2nd Gen YPM cells have similar doubling times to 1st Gen cells in mucin media, quantified during exponential growth phase from 0-1 days. All error bars denote SD. * - $p \leq 0.05$, ** - $p \leq 0.01$, *** - $p \leq 0.001$, **** - $p \leq 0.0001$.

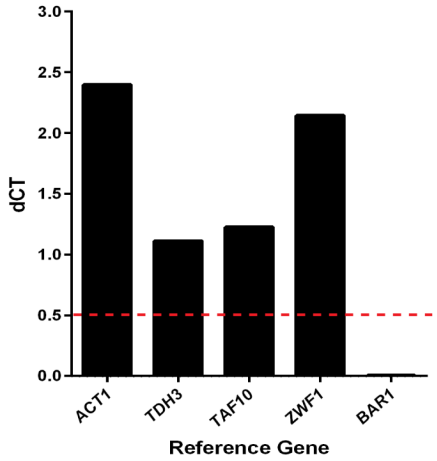

Supplemental Figure S2 *BAR1* displayed the lowest difference in gene expression between YP and YPM. WT (YKB1117) cells were grown to mid log phase in YPD, washed in YP and reinoculated into 50 mL of YP and YPM media. Cultures were incubated for 24 hrs at 30°C prior to cell harvest and normalized to the lowest concentrated culture. Cells were then lysed via beadbeating and RNA was extracted via the phenol:chloroform:isoamyl alcohol method. RNA concentration and integrity was assessed via nanodrop and gel electrophoresis. qPCR was conducted using EvaGreen and the difference in CT values between YP and YPM among various reference gene candidates were compared. The red dashed line indicates the typical cut-off (dCT ≤ 0.5) for ideal reference genes in a qPCR experiment.

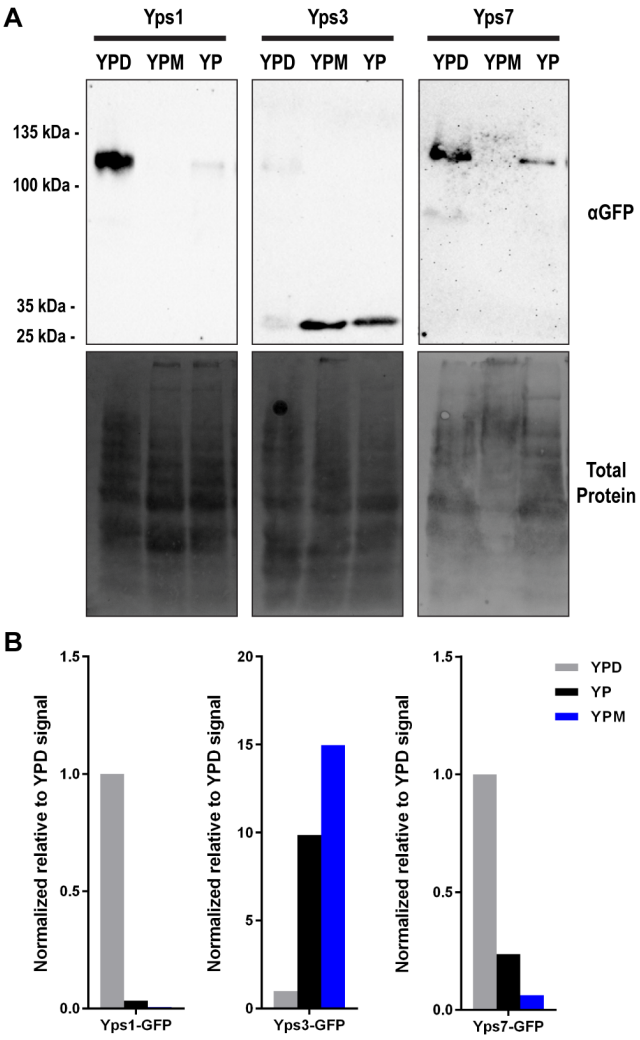

Supplemental Figure S3 Yapsin proteins are mixed in regards to abundance in mucin media. WT (YKB1079) and GFP-tagged Yps1 (YKB4901), Yps3 (YKB4902) and Yps7 (YKB4903) strains were grown to mid log phase in YPD, washed in YP and reinoculated into 500 mL of YPD, YP and YPM media. Cultures were incubated for 24 hrs prior to cell harvest. Protein extraction was conducted via TCA lysis. (B) Protein quantification of western blots for each strain in each media, normalized to YPD levels. Western blots and protein quantification are representative of one biological replicate.

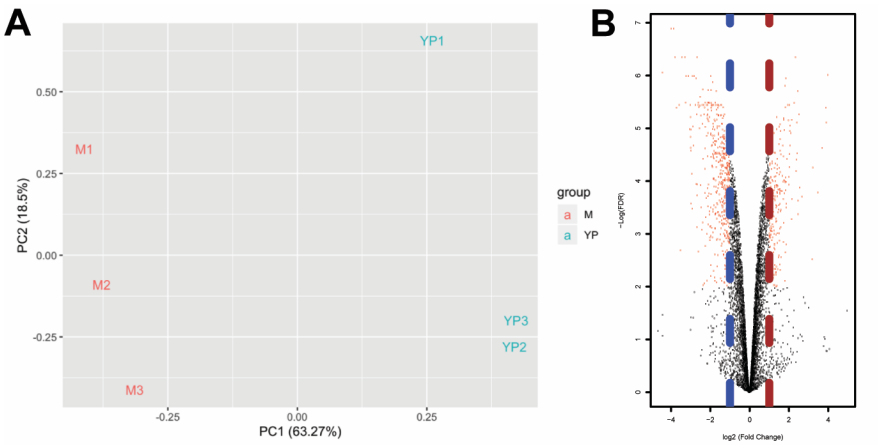

Supplemental Figure S4 Principal component analysis (PCA) and transcriptional profiling demonstrate separation by sample treatment and a large set of differentially expressed genes. (A) PCA of normalized gene counts of the first two principal components shows separation of YPM samples (red) and YP samples (green). (B) Volcano plot for all 2131 differentially expressed genes from RNA sequencing experiements. Thresholds shown here are for differential expression levels of aligned sequences calculated at log2 fold changes >1 (upregulated) and <-1 (downregulated), and an FDR adjusted p-value ≤ 0.01 (red dots).

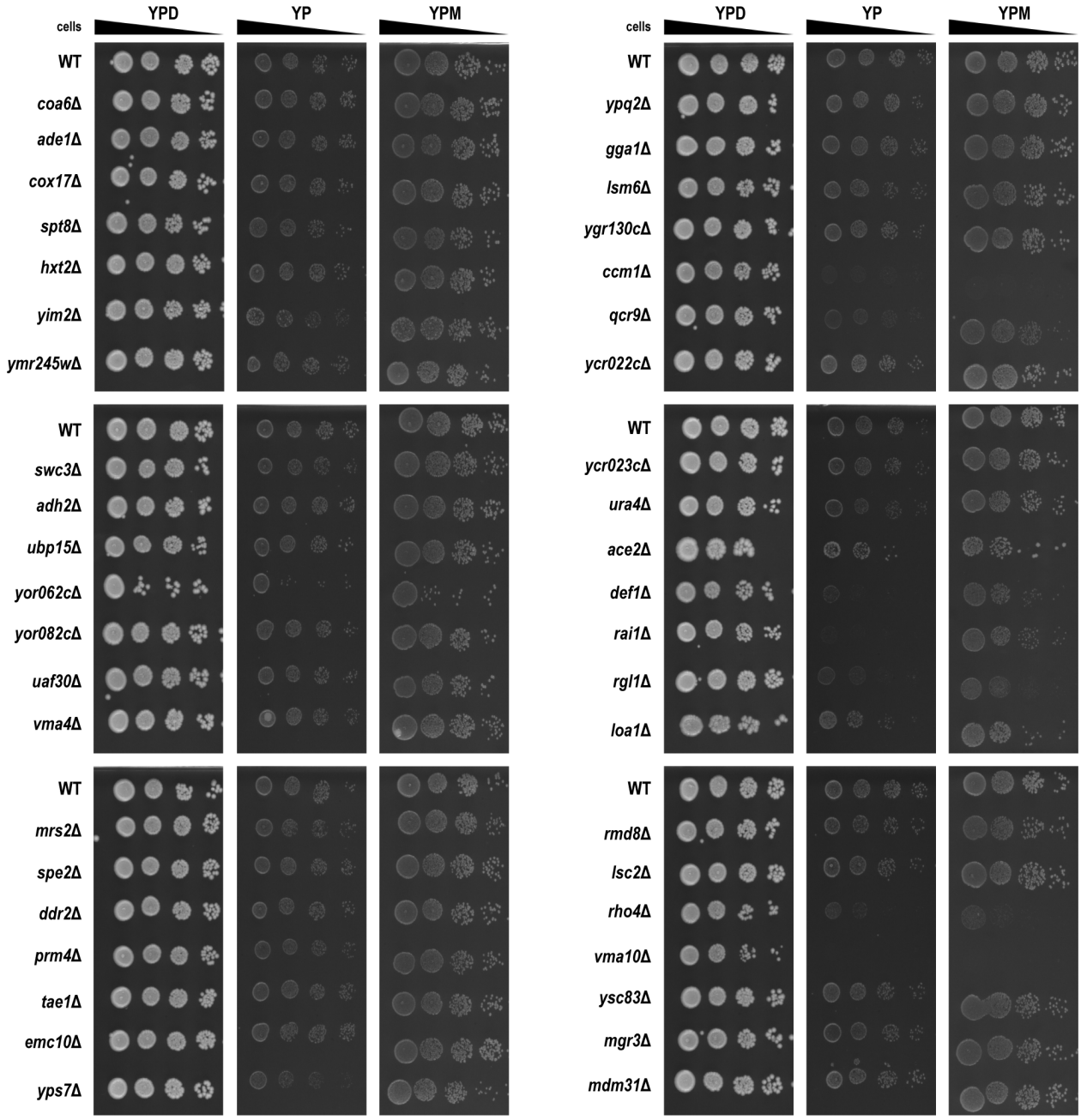
cells
YPD
YP
YPM
WT
coa6Δ
ade1Δ
cox17Δ
spt8Δ
hxt2Δ
yim2Δ
ymr245wΔ
WT
swc3Δ
adh2Δ
ubp15Δ
yor062cΔ
yor082cΔ
uaf30Δ
vma4Δ
WT
mrs2Δ
spe2Δ
ddr2Δ
prm4Δ
tae1Δ
emc10Δ
yps7Δ
cells
YPD
YP
YPM
WT
ypq2Δ
gga1Δ
lsm6Δ
ygr130cΔ
ccm1Δ
qcr9Δ
ycr022cΔ
WT
ycr023cΔ
ura4Δ
ace2Δ
def1Δ
rai1Δ
rgl1Δ
loa1Δ
WT
rmd8Δ
lsc2Δ
rho4Δ
vma10Δ
ysc83Δ
mgr3Δ
mdm31Δ

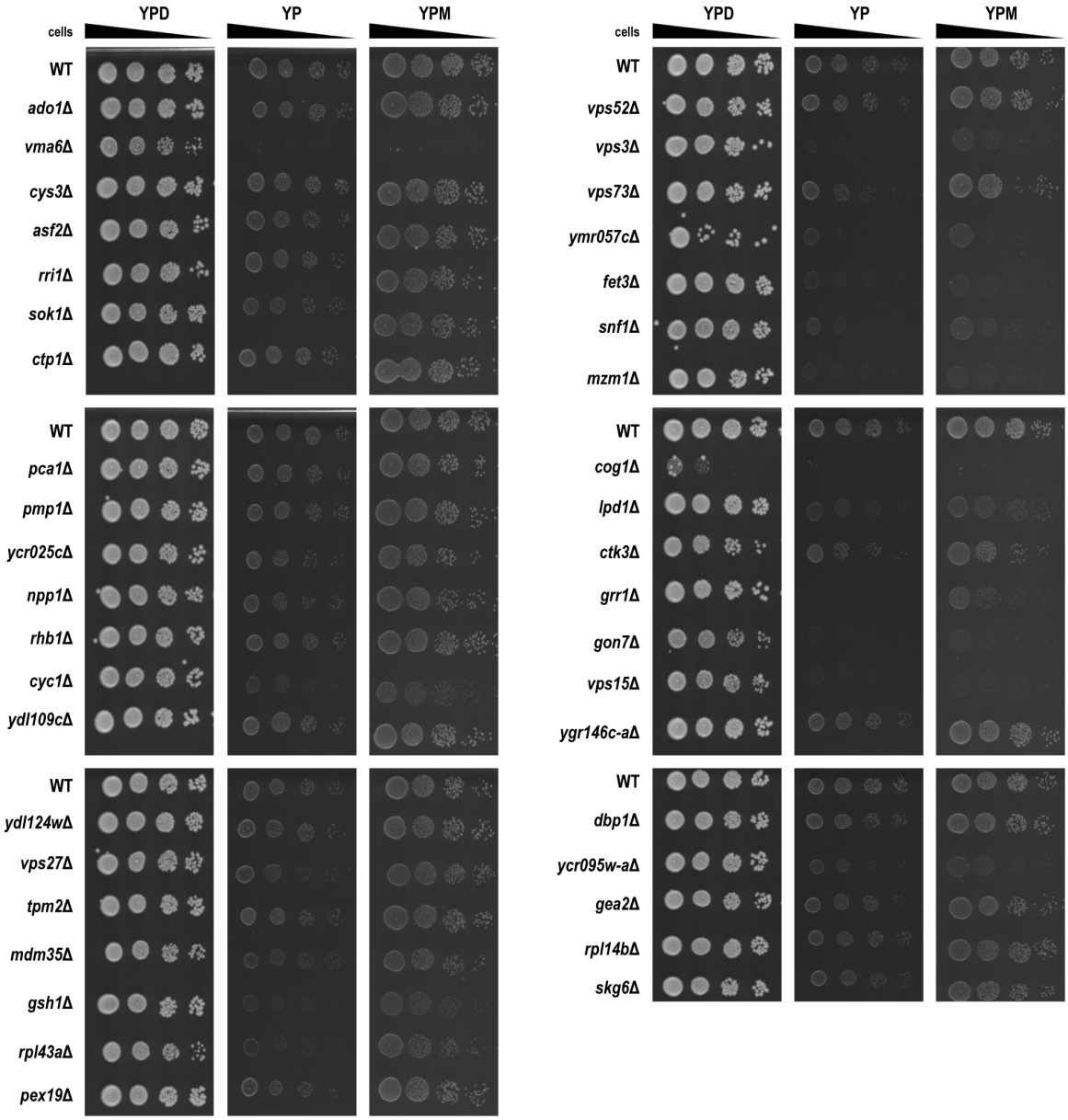

Supplemental Figure S5 Dot assay confirmations for the chemogenomics screen. WT (YKB1079), along with deletion mutant strains from the *Saccharomyces cerevisiae* deletion mutant array (DMA) were grown to mid log phase in YPD, washed in YP and diluted to a final OD600 of 0.2. Four 10-fold serial dilutions were spotted onto YPD, YP and YPM agar plates. Plates were incubated at 30°C for a duration depending on when each condensed plate had the lowest difference in average colony size between media, ranging from 2-4 days. YPM plates were condensed for figure alignment.

Supplemental Table S1 – Strain list.

Strain	Genotype	Source
YKB1079 (BY4741)	MATa his3Δ1 leu2Δ0 met15Δ0 ura3Δ0	Brachmann *et al.* (1998)[157]
YKB1117 (BY4743)	MATa his3Δ1 leu2Δ0 met15Δ0 ura3Δ0 MATα his3Δ1 leu2Δ0 lys2Δ0 ura3Δ0	Brachmann *et al.* (1998)[157]
YKB1118 (BY4742)	MATα his3Δ1 leu2Δ0 lys2Δ0 ura3Δ0	Brachmann *et al.* (1998)[157]
YKB4828	MATa his3Δ1 leu2Δ0 met15Δ0 ura3Δ0 yps1Δ::KANMX	DMA Collection (GE)
YKB4829	MATa his3Δ1 leu2Δ0 met15Δ0 ura3Δ0 yps3Δ::KANMX	DMA Collection (GE)
YKB4830	MATa his3Δ1 leu2Δ0 met15Δ0 ura3Δ0 yps5Δ::KANMX	DMA Collection (GE)
YKB4831	MATa his3Δ1 leu2Δ0 met15Δ0 ura3Δ0 yps7Δ::KANMX	DMA Collection (GE)
YKB4832	MATa his3Δ1 leu2Δ0 met15Δ0 ura3Δ0 yps6Δ::KANMX	This study
YKB4835	MATα his3Δ1 leu2Δ0 lys2Δ0 ura3Δ0 yps1Δ::NATMX	This study
YKB4836	MATα his3Δ1 leu2Δ0 lys2Δ0 ura3Δ0 yps3Δ::NATMX	This study
YKB4837	MATα his3Δ1 leu2Δ0 lys2Δ0 ura3Δ0 yps7Δ::NATMX	This study
YKB4897	MATα his3Δ1 leu2Δ0 lys2Δ0 ura3Δ0 yps1Δ::NATMX yps7Δ::KANMX	This study
YKB4898	MATα his3Δ1 leu2Δ0 lys2Δ0 ura3Δ0 yps3Δ::NATMX yps7Δ::KANMX	This study
YKB4899	MATa his3Δ1 leu2Δ0 met15Δ0 ura3Δ0 yps1Δ::KANMX yps3Δ::NATMX	This study
YKB4900	MATa his3Δ1 leu2Δ0 met15Δ0 ura3Δ0 yps1Δ::KANMX yps3Δ::NATMX yps7Δ::HYGMX	This study
YKB4901	MATa his3Δ1 leu2Δ0 met15Δ0 ura3Δ0 YPS1-GFP::HIS3	This study
YKB4902	MATa his3Δ1 leu2Δ0 met15Δ0 ura3Δ0 YPS3-GFP::HIS3	Ghaemmaghami *et al.* (2003)[109]
YKB4903	MATa his3Δ1 leu2Δ0 met15Δ0 ura3Δ0 YPS7-GFP::HIS3	Ghaemmaghami *et al.* (2003)[109]
YKB4907	MATa his3Δ1 leu2Δ0 met15Δ0 ura3Δ0 CIT1-RFP::URA3	This study
YKB4908	MATa his3Δ1 leu2Δ0 met15Δ0 ura3Δ0 ccm1Δ::KANMX	DMA Collection (GE)
YKB4912	MATa his3Δ1 leu2Δ0 met15Δ0 ura3Δ0 ycr095w-aΔ::KANMX	DMA Collection (GE)
YKB4916	MATa his3Δ1 leu2Δ0 met15Δ0 ura3Δ0 CIT1-RFP::URA3 ycr095w-aΔ::KANMX	This study
YKB4917	MATa his3Δ1 leu2Δ0 met15Δ0 ura3Δ0 slt2Δ::KANMX	DMA Collection (GE)
YKB4919	MATa his3Δ1 leu2Δ0 met15Δ0 ura3Δ0 hog1Δ::KANMX	DMA Collection (GE)
YKB4942	MATa his3Δ1 leu2Δ0 met15Δ0 ura3Δ0 CIT1-RFP::URA3 ccm1Δ::KANMX	This study
YKB5003	MATa his3Δ1 1eu2Δ0 met15Δ0 ura3Δ0 [- *LEU2*]	This study
YKB5004	MATa his3Δ1 1eu2Δ0 met15Δ0 ura3Δ0	This study

Strain	Genotype	Source
	[*HOG1* - *LEU2*]	
YKB5005	MATa his3Δ1 1eu2Δ0 met15Δ0 ura3Δ0 hog1Δ::KANMX [- *LEU2*]	This study
YKB5006	MATa his3Δ1 1eu2Δ0 met15Δ0 ura3Δ0 hog1Δ::KANMX [*HOG1* - *LEU2*]	This study
YKB5007	MATa his3Δ1 leu2Δ0 met15Δ0 ura3Δ0 yps7Δ::KANMX [- *LEU2*]	This study
YKB5008	MATa his3Δ1 leu2Δ0 met15Δ0 ura3Δ0 yps7Δ::KANMX [*HOG1* - *LEU2*]	This study
YKB5009	MATα his3Δ1 leu2Δ0 lys2Δ0 ura3Δ0 yps1Δ::NATMX yps7Δ::KANMX [- *LEU2*]	This study
YKB5010	MATα his3Δ1 leu2Δ0 lys2Δ0 ura3Δ0 yps1Δ::NATMX yps7Δ::KANMX [*HOG1* - *LEU2*]	This study
YKB5011	MATα his3Δ1 leu2Δ0 lys2Δ0 ura3Δ0 yps3Δ::NATMX yps7Δ::KANMX [- *LEU2*]	This study
YKB5012	MATα his3Δ1 leu2Δ0 lys2Δ0 ura3Δ0 yps3Δ::NATMX yps7Δ::KANMX [*HOG1* - *LEU2*]	This study
YKB5013	MATa his3Δ1 leu2Δ0 met15Δ0 ura3Δ0 yps1Δ::KANMX yps3Δ::NATMX yps7Δ::HYGMX [- *LEU2*]	This study
YKB5014	MATa his3Δ1 leu2Δ0 met15Δ0 ura3Δ0 yps1Δ::KANMX yps3Δ::NATMX yps7Δ::HYGMX [*HOG1* - *LEU2*]	This study
YKB5015	MATa his3Δ1 leu2Δ0 met15Δ0 ura3Δ0 yps2Δ::KANMX	DMA Collection (GE)

Supplemental Table S2 – Plasmid list.

Plasmid	Components	Source
PKB5	pFA6a-natMX6	Longtine *et al.* (1998)[107]
PKB6	pFA6a-kanMX6	Longtine *et al.* (1998)[107]
PKB25	pRS425	Christianson *et al.* (1992)[158]
PKB194	pFA6a-GFP(S65T)-HIS3MX6	Gift from Adam Rudner Lab (uOttawa)
PKB311	pFA6a-hphMX6	Gift from Adam Rudner Lab (uOttawa)
-	p5476-HOG1	Ho *et al.* (2009)[159]

Supplemental Table S3 – Primer list.

Primer	Sequence	Description	Source
OKB1329	5'-CTGTCAAGTTGAACAAGGAAACCAC-3'	For qPCR of *TDH3*. 5' forward internal primer 727 bp downstream of start codon.	Dacquay *et al.* (2017)[160]
OKB1330	5'-CAACGTGTTCAACCAAGTCGACAA-3'	For qPCR of *TDH3*. 3' reverse internal primer 8 bp upstream of stop codon.	Dacquay *et al.* (2017)[160]
OKB2300	5'-GCCTTCTACGTTTCCATCCA-3'	For qPCR of *ACT1*. 5' forward internal primer 387 bp downstream of start codon.	Dacquay *et al.* (2017)[160]
OKB2301	5'-CGTAAATTGGAACGACGTGA-3'	For qPCR of *ACT1*. 3' reverse internal primer 626 bp upstream of stop codon.	Dacquay *et al.* (2017)[160]
OKB2757	5'-CATCGCAGGTTCTCGGTAAG-3'	For qPCR of *YPS1*. 5' forward internal primer 43 bp downstream of start codon.	This study
OKB2758	5'-CTAGCGAGTCCCCGTAAAGC-3'	For qPCR of *YPS1*. 3' reverse internal primer 1553 bp upstream of stop codon.	This study
OKB2759	5'-AGCAGTCTTAACTAGTCCGG-3'	For qPCR of *YPS3*. 5' forward internal primer 29 bp downstream of start codon.	This study
OKB2760	5'-TCGATCTCTTGCTGAGTTCA-3'	For qPCR of *YPS3*. 3' reverse internal primer 1379 bp upstream of stop codon.	This study
OKB2761	5'-AGGAGATGTATTACGCAACA-3'	For qPCR of *BAR1*. 5' forward internal primer 118 bp downstream of start codon.	This study
OKB2762	5'-GGTAAGCAGAAGGGATTGCT-3'	For qPCR of *BAR1*. 3' reverse internal primer 1519 bp upstream of stop codon.	This study
OKB2763	5'-GATCTTCGGTTATGCCCGGT-3'	For qPCR of *ZWF1*. 5' forward internal primer 134 bp downstream of start codon.	This study
OKB2764	5'-AACTGTTCGACCTTAGAGTCA-3'	For qPCR of *ZWF1*. 3' reverse internal primer 1264 bp upstream of stop codon.	This study
OKB2765	5'-ATATTCCAGGATCAGGTCTTCCGTAGC-3'	For qPCR of *TAF10*. 5' forward internal primer 386 bp downstream of start codon.	Teste *et al.* (2009)[161]
OKB2786	5'-GCAAAGTCTGGAACCTCTTC-3'	For qPCR of *YPS7*. 5' forward internal primer 87 bp downstream of start codon.	This study
OKB2787	5'-GTTGACCGGGAGTGCCAAAT-3'	For qPCR of *YPS7*. 3' reverse internal primer 1586 bp upstream of stop codon.	This study
OKB2790	5'-GTAGTCTTCTCATTCTGTTGATGTTGTTGTTG-3'	For qPCR of *TAF10*. 3' reverse internal primer 88 bp upstream of stop codon.	Teste *et al.* (2009)[161]
OKB2839	5'-GATGATTACGAGCTGGTGGA-3'	For qPCR of *YPS2*. 5' forward internal primer 195 bp downstream of start codon.	This study

Primer	Sequence	Description	Source
OKB2840	5'-TGTCGACAAGCACAGTAACT-3'	For qPCR of *YPS2*. 3' reverse internal primer 1490 bp upstream of stop codon.	This study
OKB2841	5'-GCTGACATTGCCTATTGCAA-3'	For qPCR of *YPS5*. 5' forward internal primer 282 bp downstream of start codon.	This study
OKB2842	5'-GAGGTGGTAGTAGAACGAGG-3'	For qPCR of *YPS5*. 3' reverse internal primer 103 bp upstream of stop codon.	This study
OKB2843	5'-GCATCTTGTTTGGTGCAGTG-3'	For qPCR of *YPS6*. 5' forward internal primer 781 bp downstream of start codon.	This study
OKB284*	5'- ATCCCAGGATTTGAGCCAAG -3'	For qPCR of *YPS6*. 3' reverse internal primer 727 bp upstream of stop codon.	This study

Supplemental Table S4 – Top screen hits resulting in a positive impact on growth in YPM compared to YP upon their deletion.

Systematic Name	Gene Name	YPM/YP Ratio (Approach 1[a])	YPM/YP Ratio (Approach 2[b])
YGR183C	QCR9	2.09	3.51
YLR131C	ACE2	2.07	2.07
YGL246C	RAI1	1.96	2.07
YJL101C	GSH1	1.92	3.87
YMR245W	YMR245W	1.81	1.89
YOR082C	YOR082C	1.79	1.79
YDR349C	YPS7	1.76	1.81
YGR244C	LSC2	1.72	1.68
YLR420W	URA4	1.70	1.67
YJR090C	GRR1	1.68	1.76
YEL022W	GEA2	1.67	1.41
YDR006C	SOK1	1.66	1.81
YGR130C	YGR130C	1.66	1.66
YPR139C	LOA1	1.64	1.91
YCR022C	YCR022C	1.63	1.65
YGR150C	CCM1	1.61	1.57
YKL054C	DEF1	1.60	2.35
YDR493W	MZM1	1.60	1.61
YDR358W	GGA1	1.59	1.61
YDR056C	EMC10	1.59	1.62
YLR447C	VMA6	1.58	2.50
YPR043W	RPL43A	1.58	1.56
YJR105W	ADO1	1.58	1.61
YCR023C	YCR023C	1.57	1.56
YBR261C	TAE1	1.57	1.58
YDR352W	YPQ2	1.56	1.56
YPL119C	DBP1	1.56	1.56
YMR244C-A	COA6	1.56	1.60
YHL001W	RPL14B	1.56	1.83
YDR378C	LSM6	1.56	1.56
YKL053C-A	MDM35	1.54	2.86
YPL156C	PRM4	1.33	2.15
YHR039C-B	VMA10	1.21	2.11
YJR048W	CYC1	1.49	1.99
YHR149C	SKG6	1.41	1.88
YOR295W	UAF30	1.47	1.88
YMR011W	HXT2	1.34	1.88
YLR055C	SPT8	1.52	1.87
YLL009C	COX17	1.39	1.86
YOR062C	YOR062C	1.35	1.78
YGR146C-A	YGR146C-A	1.39	1.75
YMR115W	MGR3	1.52	1.72
YMR151W	YIM2	1.50	1.68
YGL104C	VPS73	1.14	1.68
YDL065C	PEX19	1.50	1.68

[a] – average ratio of average colony size on YPM to YP for each strain.
[b] – average of the average ratio of each pinned colony size on YPM to YP for each strain.

Supplemental Table S5 – Top screen hits resulting in a negative impact on growth in YPM compared to YP upon their deletion.

Systematic Name	Gene Name	YPM/YP Ratio (Approach 1[a])	YPM/YP Ratio (Approach 2[b])
YNR006W	VPS27	0.30	0.53
YBR097W	VPS15	0.53	0.47
YOR334W	MRS2	0.56	0.57
YMR304W	UBP15	0.63	0.66
YMR058W	FET3	0.64	0.66
YFR048W	RMD8	0.67	0.82
YPL066W	RGL1	0.67	0.67
YMR303C	ADH2	0.67	0.72
YAL012W	CYS3	0.69	0.78
YGL223C	COG1	0.70	0.73
YMR057C	YMR057C	0.70	0.73
YML112W	CTK3	0.71	0.71
YKR055W	RHO4	0.71	0.71
YAR015W	ADE1	0.71	0.73
YDR477W	SNF1	0.71	0.60
YHR017W	YSC83	0.72	0.66
YDL197C	ASF2	0.72	0.71
YCR026C	NPP1	0.73	0.73
YJL184W	GON7	0.74	1.06
YDL109C	YDL109C	0.74	0.76
YCR095W-A	YCR095W-A	0.74	0.75
YHR194W	MDM31	0.74	0.70
YOR332W	VMA4	0.75	0.77
YDL216C	RRI1	0.75	0.67
YAL011W	SWC3	0.76	0.82
YBR291C	CTP1	0.76	0.79
YOL052C	SPE2	0.76	0.83
YOL053C-A	DDR2	0.76	0.85
YCR027C	RHB1	0.76	0.71
YDL124W	YDL124W	0.76	0.72
YCR025C	YCR025C	0.89	0.68
YFL018C	LPD1	1.43	0.70
YDR484W	VPS52	0.77	0.71
YCR024C-A	PMP1	0.92	0.74
YBR295W	PCA1	0.77	0.75
YDR495C	VPS3	0.76	0.77
YIL138C	TPM2	0.76	0.77

[a] – average ratio of average colony size on YPM to YP for each strain.
[b] – average of the average ratio of each pinned colony size on YPM to YP for each strain.

9.0 Curriculum Vitae

Kevin Mercurio

EDUCATION

Master of Science in Biochemistry **Sept 2017 — Apr 2020**
University of Ottawa **Ottawa, Ontario**
- Thesis Title: Identifying genes required for *Saccharomyces cerevisiae* growth in mucin.
- Supervisor: Dr. Kristin Baetz

Honours Bachelor of Science, Major in Biochemistry (with Co-op) **Sept 2011 — Jun 2016**
University of Ottawa **Ottawa, Ontario**

RESEARCH EXPERIENCE

Graduate Student **Sept 2017 — Apr 2020**
University of Ottawa **Ottawa, Ontario**
- Utilized genetics and microscopy tools to determine how yeast can metabolize mucin as an energy source, such as how fungi survive in the human gut.
- Performed chemogenomics screening of the *Saccharomyces cerevisiae* Deletion Mutant Array, and RNA sequencing that lead to the identification of important genes for growth in mucin.
- Expanded oral presentation skills through powerpoints and posters showcasing project findings.

Undergraduate Student (Honours) **Sept 2015 — Aug 2016**
University of Ottawa **Ottawa, Ontario**
- Investigated biofilm-specific antibiotic resistance in *Pseudomonas aeruginosa* commonly found in cystic fibrosis individuals using minimal bactericidal concentration assays on transposon-insertion mutants.
- Conducted qPCR analysis comparing gene expression between biofilm and planktonic cells.
- Constructed gene deletion mutants via plasmid manipulation and gene recombination.

Co-op Researcher **Sept 2014 — Dec 2014**
FPInnovations **Montreal, Quebec**
- Enhanced the efficiency of enzymatic hydrolysis on softwood paper pulp material, as a means to obtain useful sugars for biochemical synthesis.
- Utilized cellulases, hemicellulases and performance-enhancing additives (acids, sulfites) to break down problematic lignin biomass, leading to optimal product formation.
- Developed strong communication skills through presentations to company superiors.

Co-op Researcher **May 2014 — Aug 2014**
University of Alberta **Edmonton, Alberta**
- Developed a robust method for spectrophotometric quantification of phage virulence.
- Established 96-well plate virulence assay protocols using different infection conditions by varying parameters like temperature, adsorption efficiency and infection media.
- Participated in a poster symposium communicating overall findings and future avenues to university personnel and fellow research interns.

ANALYTICAL AND PROFESSIONAL TRAINING

Technologies for Microbiome Science and Engineering (TechnoMiSE)
- Part of the Natural Science and Engineering Research Council of Canada's Collaborative Research and Training Experience Programs (NSERC-CREATE).
- Developed bioinformatics skills in workshops about the analysis of large datasets via RStudio.
- Advanced science communication skills through practicing oral presentations and networking with industry partners in microbiome science.
- Expanded on skills such as time-management, productivity, stress management and work-life balance through professional Mitacs workshops.
- To encourage trainee participation in program development, organized the TechnoMiSE Student Committee for trainee networking and project support.

PUBLICATIONS AND PRESENTATIONS

Peer-Reviewed Publications
- Storms Z., Teel M., **Mercurio K.**, Sauvageau D. (2019). The Virulence Index: A Metric for Quantitative Analysis of Bacteriophage Virulence. *PHAGE: Therapy, Applications, and Research, 1: 1X*. Invited article for the preview/inaugural issues
- Fletcher E., Gao K., **Mercurio K.**, Ali M., Baetz K. (2019). Yeast chemogenomic screen identifies distinct metabolic pathways required to tolerate exposure to phenolic fermentation inhibitors ferulic acid, 4-hydroxybenzoic acid and coniferyl aldehyde. *Metabolic Engineering, 52: 98-109*.

Research Posters and Oral Presentations
- **Mercurio K.** (2019). *Identifying genes required for Saccharomyces cerevisiae growth in mucin*. Presentation for the International Conference on Yeast Genetics and Molecular Biology, Gothenburg, Sweden.
- **Mercurio K.**, Singh D., Baetz K. (2019). *Identifying genes required for Saccharomyces cerevisiae growth in mucin*. Primary author of poster for the Ottawa Institute of Systems Biology Conference, Cornwall, Ontario, Canada.
- **Mercurio K.**, Hall C. W., Mah T. F. (2016). *Identification of a novel gene involved in Pseudomonas aeruginosa biofilm-specific resistance to antibiotics*. Primary author of poster for the Canadian Society of Microbiologists' Conference, Toronto, Ontario, Canada.

HONOURS AND AWARDS

- Winner of M. Sc. Biochemistry Seminar Day (uOttawa, 2019)
- Graduate Studies Leadership Award for Student Engagement (uOttawa, 2018)
- *Cum laude* undergraduate academic honours (uOttawa, 2016)
- NSERC Industrial Undergraduate Student Research Award (2014)
- Entrance scholarship valued at $8,000 (uOttawa, 2011-2012)
- Ontario Scholar Award (St. Paul Catholic High School, 2011)

OTHER PROFESSIONAL EXPERIENCE

Trade Commissioner **Nov 2016 — Aug 2017**
Global Affairs Canada **Ottawa, Ontario**
- Mandate is to support the Canadian biopharmaceutical and biotechnology sector.

- Contact company administration for sector insight and support in business development.
- Design technical reports and presentations about the Canadian impact in emerging fields such as immune-oncology and gene therapy.
- Participate in interdepartmental sector discussions and government conferences.

Junior Trade Commissioner (Co-op) **Jun 2015 — Aug 2015**
Global Affairs Canada **Ottawa, Ontario**
- Gathered intel on the domestic activity of the Canadian Life Sciences industry.
- Acquired fundamental understanding of the fields of immuno-oncology, gene therapy and autoimmune disease for the division.
- Collaborated with team members to design reports and presentations for the division.

Risk Profiler (Co-op) **Jan 2014 — Apr 2014**
Canadian Food Inspection Agency **Ottawa, Ontario**
- Gathered and organized massive amounts of information as a basis for food safety reports.
- Assessed the severity of chemical and biological hazards prevalent in common Canadian food items, such as cadmium in rice products and lead in tea leaves.

VOLUNTEER EXPERIENCE

Mentorship Coordinator **Sept 2019 — *present***
Science to Business Network (S2BN) **Ottawa, Ontario**
- To bridge the gap between science and industry, created the inaugural S2BN Mentorship program for STEM-based graduate students and post-doctoral fellows in the Ottawa region.
- Created promotional materials, organized call for applications and conducted matchmaking between trainees and governmental/industry professionals.

Student Representative **Nov 2017 — Aug 2019**
Faculty of Medicine Graduate Student Recruitment Committee **Ottawa, Ontario**
- Supports administration in developing strategies to encourage recruitment to the Faculty of Medicine's graduate programs.
- Major role in the development of the Faculty's DEGREE Shadowing Program for local and provincial undergraduate students.

Student Committee Leader **Oct 2017 — Aug 2019**
TechnoMiSE Student Association **Ottawa, Ontario**
- Supports the communication between program coordinators and program trainees.
- Encourages interpersonal and networking skill development through the organization of social events between trainees.

Vice-President of Academic Affairs **May 2018 — April 2019**
Biochemistry, Microbiology & Immunology Graduate Student Association **Ottawa, Ontario**
- Represented graduate students both at the departmental and faculty level.
- Communicated academic feedback to department program directors and administration while relaying important information back to the students.
- Organized academic-related events throughout the school year such as scientific panels, skills workshops and Faculty of Medicine's Career Day.
- To address student confusion about educational and research issues, worked with the faculty administration to design orientation workshops for trainees.
- Actively engaged the student community through the organization of social events.

In-School Mentor **Oct 2015 — Jun 2016**
Big Brothers Big Sisters **Ottawa, Ontario**
- Supervised a Little brother at his elementary school on a weekly basis.
- Designed activities to develop communication and creativity skills.
- Signified the importance of education and developing positive relationships with family, friends and members in the community.

Vice-President of Social Affairs **Sept 2015 — Apr 2016**
University of Ottawa Healthcare Symposium **Ottawa, Ontario**
- Organized the largest conference at the university directed towards the challenges of a frequently changing healthcare field.
- Responsible for coordinating volunteer teams and planning event catering.
- Managed social events and activities, such as designing the "Socrates Cafe" event for discussion amongst attendees on relevant healthcare issues.

Student Educator **Sept 2015 — Apr 2016**
University of Ottawa Health Services **Ottawa, Ontario**
- Member of Leave The Pack Behind (LTPB): an Ontario university tobacco information program.
- Informed the student body about health-related services and events offered by the organization through in-person interactions.
- Organized events such as CO-testing and contests with the intent of providing information on the disadvantages of all types of smoking, and the benefits of quitting or reducing.

OTHER INFORMATION

- **ORCID:** https://orcid.org/0000-0002-3126-5509
- **LinkedIn:** https://ca.linkedin.com/in/kevin-mercurio-36741080
- **TechnoMiSE Profile:** http://create-technomise.ca/kevin-mercurio/
- **Website:** https://www.kjbmercurio.com/
- **Twitter:** @kjbmercurio

REFERENCES

Available upon request.